Atmos. Chem. Phys. Discuss., https://doi.org/10.5194/acp-2018-1172
Manuscript under review for journal Atmos. Chem. Phys.
Discussion started: 17 December 2018

Atmospheric Chemistry and Physics Discussions

Emission of volatile halogenated organic compounds over various landforms at the Dead Sea

Moshe Shechner[1] Alex Guenther[2], Robert Rhew[3], Asher Wishkerman[4], Qian Li[1], Donald Blake[2], Gil Lerner[1] and Eran Tas[1]*

[1]The Robert H. Smith Faculty of Agricultural, Food & Environment, Department of Soil and Water Sciences, The Hebrew University of Jerusalem, Rehovot, Israel
[2]Department of Earth System Science, University of California, Irvine, CA, USA; Department of Geography at Berkeley
[3] Department of Geography and Berkeley Atmospheric Sciences Center, University of California, Berkeley, Berkeley, California 94720, United States
[4]Ruppin Academic Center, Michmoret, Israel; Department of Chemistry, University of California, Irvine, Irvine, CA 92697

[*] Corresponding author –Eran Tas, The Department of Soil and Water Sciences, The Robert H. Smith Faculty of Agriculture, Food and Environment, Hebrew University of Jerusalem, Rehovot, Israel. eran.tas@mail.huji.ac.il.

Atmos. Chem. Phys. Discuss., https://doi.org/10.5194/acp-2018-1172
Manuscript under review for journal Atmos. Chem. Phys.
Discussion started: 17 December 2018

Atmospheric Chemistry and Physics Discussions

Abstract. Volatile halogenated organic compounds (VHOCs), such as methyl halides (CH_3X; X=Br, Cl and I) and very short-lived halogenated substances (VSLS; $CHBr_3$, CH_2Br_2, $CHBrCl_2$, C_2HCl_3, $CHCl_3$ and $CHBr_2Cl$) are well known for their significant influence on ozone concentrations and oxidation capacity of the troposphere and stratosphere, and for their key role in aerosol formation. Insufficient characterization of the sources and emission rate of VHOCs limits our present ability to understand and assess their impact in both the troposphere and the stratosphere. Over the last two decades several natural terrestrial sources for VHOCs, including soil and vegetation, have been identified, but our knowledge about emission rates from these sources and their responses to changes in ambient conditions remains limited. Here we report measurements of the mixing ratios and the fluxes of several chlorinated and brominated VHOCs from different landforms and vegetated sites at the Dead Sea during different seasons. Fluxes were highly variable but were generally positive (emissive), corresponding with elevated mixing ratios for all of the VHOCs investigated in the four investigated site types — bare soil, coastal, cultivated and natural vegetated sites — except for fluxes of CH_3I and C_2HCl_3 over the vegetated sites. In contrast to previous reports, we also observed emissions of brominated trihalomethanes, with net molar fluxes ordered as follows: $CHBr_2Cl$ > $CHBr_3$ > $CHBrCl_2$ > $CHCl_3$. This finding can be explained by the enrichment of soil with Br. Correlation analysis, in agreement with recent studies, indicated common controls for the formation and emission of all the above trihalomethanes but also for CH_2Br_2. Also in line with previous reports, we observed elevated emissions of $CHCl_3$ and C_2HCl_3 from mixtures of soil and different salt-deposited structures; the high correlations of flux with methyl halides, and particularly with CH_3I, suggested that at least CH_3I is also emitted via similar mechanisms or is subjected to similar controls. Overall, our results indicate elevate emission of VHOCs from bare soil under semi-arid conditions. Along with other recent studies, our findings point to the strong emission potential of a suite of VHOCs from saline soils and salt lakes, and call for additional studies of emission rates and mechanisms of VHOCs from saline soils and salt lakes.

Atmos. Chem. Phys. Discuss., https://doi.org/10.5194/acp-2018-1172
Manuscript under review for journal Atmos. Chem. Phys.
Discussion started: 17 December 2018

1 Introduction

Volatile halogenated organic compounds (VHOCs), such as methyl halides (CH_3X; X=Br, Cl and I) and very short-lived halogenated substances (VSLS) contribute substantially to the loading of tropospheric and lower stratospheric reactive halogen species (RHS, containing Cl, Br or I and their oxides) (Carpenter and Reimann et al., 2014;Carpenter et al., 2013;Derendorp et al., 2012). RHS in turn lead to destruction of ozone (O_3), changes in atmospheric oxidation capacity, and radiative forcing (Simpson et al., 2015). Depletion of O_3 in the stratosphere is associated with damage to biological tissues owing to an increase in transmittance of UVB radiation (Rousseaux et al., 1999). In the troposphere O_3 depletion is of great importance, given that O_3 is toxic to humans, plants, and animals, is a greenhouse gas, and plays a key role in the oxidation capacity of the atmosphere.

Owing to their relatively short lifetimes (<6 months) the transport of VSLS to the stratosphere occurs primarily in the tropics, where deep convection is frequent. Brominated VSLS primarily originate from the ocean whereas chlorinated VSLS, except for $CHCl_3$ and C_2H_5Cl, originate primarily from anthropogenic sources. CH_3I, having a relatively short lifetime, is also classified as a VSLS, and contributes significantly to tropospheric O_3 destruction in the marine boundary layer (MBL) (Carpenter and Reimann et al., 2014) and also, indirectly, to cloud condensation nuclei formation (O'Dowd et al., 2002). It is now well established that emission of brominated (e.g., $CHBr_3$, CH_2Br_2, and $CHClBr_2$) and iodinated (e.g., CH_3I) VSLS tends to be much larger in coastal areas than in the open ocean (Carpenter et al., 2009;Carpenter et al., 2000;Liu et al., 2011;Bondu et al., 2008;Manley and Dastoor, 1988;Quack and Wallace, 2004), since in the former they can also be emitted from macroalgae under oxidative stress at low tide (Pedersen et al., 1996). The ocean is also a major source of CH_3Br, and a significant (~19 %) source of CH_3Cl (Carpenter and Reimann et al., 2014), as they originate from phytoplankton, bacteria, and detritus.

Atmos. Chem. Phys. Discuss., https://doi.org/10.5194/acp-2018-1172
Manuscript under review for journal Atmos. Chem. Phys.
Discussion started: 17 December 2018

Despite the numerous efforts made in recent years to evaluate halocarbon budgets, uncertainties still exist concerning the strengths of both their sources and their sinks. The budgets of CH_3Br and CH_3Cl are unbalanced, with sinks outweighing sources by ~32 % and ~17 %, respectively (Carpenter and Reimann et al., 2014). Uncertainties in the global budgets of naturally occurring VSLS are large, with discrepancies having a factor of ~2−3 between top-down and bottom-up emission inventories (Carpenter and Reimann et al., 2014). This results largely from poor characterisation of emission sources (Warwick et al., 2006;Hossaini et al., 2013;Ziska et al., 2013).

Studies over the past few decades have clearly demonstrated that terrestrial sources also constitute a major fraction of the atmospheric budget for both methyl halides and VSLS (Carpenter and Reimann et al., 2014). Many terrestrial plants have been identified as sources of CH_3Cl (Yokouchi et al., 2007), and the results of recent modelling indicate that about 55 % of the global sources of CH_3Cl originate from tropical lands (Xiao et al., 2010;Carpenter and Reimann et al., 2014). It was also suggested that natural terrestrial sources of CH_3Br, especially emissions from terrestrial vegetation, must account for a large part of the missing sources (Gebhardt et al., 2008;Yassaa et al., 2009;Warwick et al., 2006;Gan et al., 1998;Yokouchi et al., 2002;Moore, 2006;Rhew et al., 2001;Wishkerman et al., 2008), and emissions have been observed from peatlands, wetlands, salt marshes, shrublands, forests, and some cultivated crops (Gan et al., 1998;Varner et al., 1999;Lee-Taylor and Holland, 2000). $CHCl_3$ was also found to be emitted from various terrestrial sources, including rice, soil, tundra, forest floor, and different types of microorganisms such as fungi and termites (see Dimmer et al. (2001) and (Rhew et al., 2008)).

The importance of VHOC emission from soil, sediments, and salt lake deposits was recently recognized (see Kotte et al. (2012), Ruecker et al. (2014), and references therein). For example, Keppler et al. (2000) revealed natural abiotic emission of CH_3Br, CH_3Cl, and CH_3I as well as additional chlorinated VHOCs from soil and sediments harboring an oxidant such as Fe(III),

halides, and organic matter (OM), while Weissflog et al. (2005) found that salt lake sediments can be a source for several C1 and C2 chlorinated species, including $CHCl_3$ and C_2HCl_3, induced by halobacteria in the presence of dissolved Fe. Huber et al. (2009) identified an abiotic natural emission of trihalomethanes from soil, including $CHCl_3$, $CHBrCl_2$, and $CHBr_2Cl$, induced by oxidation of OM by Fe(III) and hydrogen peroxide, while Hoekstra et al. (1998) identified natural emission of $CHBr_3$ following enrichment of the soil by KBr. In addition, Carpenter et al. (2005) identified $CHBr_3$ emission from a peatland or another terrestrial source at Mace Head. Albers et al. (2017) revealed that $CHCl_3$, $CHBrCl_2$, and potentially also other trihalomethanes can be emitted from soils, probably induced by hydrolysis of trihaloacetyl compounds. Several other studies report strong emissions of CH_3Cl, CH_3Br, and CH_3I from coastal marsh vegetation and to a lesser extent from the marsh's soil (Rhew et al., 2002;Rhew et al., 2001;Rhew et al., 2014;Wishkerman et al., 2008;Rhew et al., 2000), with significant importance on a global scale (Deventer et al., 2018;Manley et al., 2006). In addition, peatland has been indicated as an important source for CH_3Br, CH_3Cl, CH_3I and $CHCl_3$ (Simmonds et al., 2010;Khan et al., 2012;Dimmer et al., 2001;Carpenter et al., 2005), and Sive et al. (2007) identified a globally significant source of CH_3I from mid-latitude vegetation and soil.

Accordingly, the need for improved understanding of VHOC emission from saline environments and their potential importance on the global scale have been highlighted by recent studies (Weissflog et al., 2005;Kotte et al., 2012;Ruecker et al., 2014;Deventer et al., 2018). Moreover, owing to global warming, saline environments are likely to become more prevalent (IPCC 2007;Ruecker et al., 2014). The present study is aimed at improving our knowledge about the emission of VHOCs from salt lake environments by quantifying the flux and the mixing ratios of methyl halides and halogenated VSLS from different sites in the area of the Dead Sea.

The Dead Sea is unique because it is the lowest point on the Earth's surface, about 430 m below sea level, with water salinity and $[Br^-]/[Cl^-]$ ratio 12 and 7.5 times higher than in normal ocean waters, respectively. Fast evaporation from the sea leads to a variety of newly exposed

landforms. Despite the high salinity, emission of VHOCs via biotic processes at the Dead Sea is also potentially feasible. The unicellular green alga *Dunaliella parva* was found to be active in Dead Sea water (Oren and Shilo, 1985), while additional bacteria and fungi that were isolated from the sea could also potentially be active under the extreme conditions (Oren et al., 2008;Jacob et al., 2017;Buchalo et al., 1998). Mycobiota, including fungi and biota, were also detected in the Dead Sea's hypersaline soil and coastal sand (Pen-Mouratov et al., 2010;Kis-Papo et al., 2001;Jacob et al., 2017).

Studying the emission of VHOCs at the Dead Sea is also interesting, in view of local sharp ozone depletion events (Hebestreit et al., 1999;Tas et al., 2003;Matveev et al., 2001;Zingler and Platt, 2005;Tas et al., 2006) as well as mercury depletion events (Tas et al., 2012;Obrist et al., 2011) in the boundary layer at this area. Emissions of brominated and iodinated VSLS can potentially lead to formation of the reactive iodine and bromine species that are responsible for these processes.

2 Methods

2.1 Field measurements and samplings

Field measurements were taken at selected sites along the Dead Sea to measure the mixing ratios and evaluate the vertical flux of VHOCs over different land-use types, seasons, and distance from the seawater, as summarized in Table 1. Soil samples from the various sites were analyzed and meteorological measurements were performed in situ, as described below.

2.1.1 Measurement sites

All measurements were taken at the Dead Sea area. The Dead Sea's geographic position is between 31°50' N and 31°00' N, 35°30' E, about 430 m below sea level. It is located in a semi-arid area with a very high seawater evaporation rate of 400 cm y^{-1} (Alpert et al., 1997), and has only a low rate of freshwater inflow. As a result, the water salinity is 12 times higher than that

Atmos. Chem. Phys. Discuss., https://doi.org/10.5194/acp-2018-1172
Manuscript under review for journal Atmos. Chem. Phys.
Discussion started: 17 December 2018

of normal ocean water. Dead Sea water contains on average 5.6 g L^{-1} bromide and 225 g L^{-1} chloride (Br^-/Cl^- ratio ≈ 0.025) (Niemi, 1997), whereas normal ocean water contains 0.065 g L^{-1} bromide and 19 g L^{-1} chloride (Br^-/Cl^- ratio ≈ 0.0034) (Sverdrup, 1942).

All measurement sites are nearly flat and are located either along or near the Dead Sea coast (see Fig. 1). Overall, for our investigations we selected emissions from bare soil sites (BARE) at Mishmar (MSMR; BARE−MSMR) and at Massada (MSD; BARE−MSD), coastal sites that are mixtures of soil and salt deposits (COAST) at Ein-Gedi (EGD; COAST−EGD) and Tzukim (TKM; COAST−TKM), natural Tamarix vegetation at Ein Tamar (ET; TMRX−ET), cultivated watermelon agricultural field at Kalya (KLY; WM−KLY), and directly from the seawater at Kedem (KDM; SEA−KDM). Note that at SEA−KDM we did not evaluate fluxes. Based on in-situ wind direction measurements, the sampled air masses at SEA−KDM were transported over the seawater from the east (see Fig. 1), at least 1 h prior to sampling and during the sampling. To study the effect of distance from the seawater on emission rates, measurements at both COAST−EGD and COAST−TKM were taken at three and two different distances from the sea, respectively. The shorter, middle, and longer distances from the seawater are termed, respectively, SD, MD and LD. Emission rates at both COAST−EGD and COAST−TKM could potentially be affected by the distance from the seashore; there are several reasons for this, including changes across the sites in salt and water soil content and changes in density of the extremely sparse vegetation cover. In addition, depending on the local wind direction at COAST−TKM-SD and COAST−EGD-SD, direct emission and uptake from the seawater can potentially affect the samplings.

In the following we briefly describe the different measurement sites, while additional information about the sites and measurements is provided in Table 1. BARE−MSMR has a bare soil consisting of loess and a small fraction of drifted soil covered with small stones and extremely sparse vegetation, and is located in a valley 1.5 km to the west of the Dead Sea shore. MSD has bare Hamada soil, with small stones and loess, and is located 2.1 km to the west of the

Dead Sea. COAST−EGD-SD has a dried-out bare saline soil, mixed with salty beds and rocks and obtaining a small contribution of fresh water inflow at the Dead Sea shore. COAST−EGD-MD has a dried-out sea bed of bare saline soil, mixed with salty beds and rocks, 0.3 km west of the Dead Sea shore. COAST−EGD-LD is a dried-out sea bed of loess saline bare soil, mixed with drifted soil, 0.8 km from the Dead Sea shore. COAST−TKM-SD is a wetted bare soil with salt deposits, groundwater inflow from the Dead Sea, and minor (<5 %) fresh water inflow lines covered with perennial grasses found in wetlands (e.g., *Phragmites* sp.), about 0.5 km from the shore. COAST−TKM-LD is a flat rocky loess area about 1.5 km from the shore, with patchy salts and sparse mixed shallow vegetation including mostly small *Atriplex* sp., *Tamarix* sp. and *Retama raetam*. TMRX−ET is a moderately dense *Tamarix* shrubland, with sandy soil, located 1.7 km south of the southern tip of the Dead Sea evaporation ponds. WM−KLY is a well-irrigated flat cultivated watermelon agricultural field located 2.5 km NW of the Dead Sea shore.

2.1.2 Field measurements and sampled air analysis

Air was sampled at each site by placing three different canisters at specified heights (see Table 1) along a meteorological tower. The samples were used to quantify the mixing ratios of different VHOCs in the air, and their corresponding fluxes calculated by applying the flux-gradient method (see (Stull 1988;Maier and Schack-Kirchner, 2014;Meredith et al., 2014)). All canisters were placed high enough above the ground to ensure that all samplings were performed within the inertial sublayer, except for the lowest canister at TMRX−ET. To minimize non-synchronized air sampling by the three canisters, we constructed a special system that allows a fast and almost simultaneous lifting of the canisters. Facilitated by passive grab samplers (RESTEK Corporation, PA, U.S.), we performed each sampling within 20 minutes by pulling air into evacuated 1.9 L stainless steel canisters, resulting in an internal canister pressure higher than 600 torr. Meteorological parameters, including temperature and relative humidity, wind speed and direction, and global solar radiation, were all continuously measured, starting at

least 30 min before air sampling was initiated. All canisters were sent to the Blake/Rowland group, University of California, Irvine (UCI), where they were subjected to the analytical techniques described in detail in Colman et al. (2001). Analyses were performed using gas chromatography combined with mass spectrometry, flame ionization detection and electron capture detection to quantify the air mixing ratios of bromoform ($CHBr_3$), trichloroethene (C_2HCl_3), methylene bromide (CH_2Br_2), dibromochloromethane ($CHBr_2Cl$), bromodichloromethane ($CHBrCl_2$), trichloroethene (C_2HCl_3), chloroform ($CHCl_3$), methyl iodide (CH_3I), methyl bromide (CH_3Br) and methyl chloride (CH_3Cl). For all gases, accuracy ranged between 1 % and 10 % and analytical precision between 1 % and 5 % (see Table S1). Note that the mid-height canister analysis of TMRX−ET-1 indicated a mixing ratio for CH_3Cl that seemed not to agree with any other measured mixing ratios for this species. We therefore excluded this measurement from all our calculations and used only the lowest and the highest canisters in the flux calculation for TMRX−ET−1, which may reflect less accurate flux evaluation. This potentially less accurate flux evaluation is indicated in all relevant figures and tables.

Atmos. Chem. Phys. Discuss., https://doi.org/10.5194/acp-2018-1172
Manuscript under review for journal Atmos. Chem. Phys.
Discussion started: 17 December 2018

Atmospheric Chemistry and Physics Discussions

Table 1. Summary of volatile halogenated organic compounds over the Dead Sea. The table records the date, time, site name (and abbreviation), sampling height, and whether the sampling could potentially be influenced by emission from the seawater and by precipitation prior to sampling.

Date dd/m/yyyy	Time (Local)	Site name / measurement abbreviation [a]	Sampling heights (m)	Seawater [b]	Precipitation (days before sampling) [c]
20/4/2016	08:45−08:55	BARE−MSMR / BARE−MSMR-1	2.5, 4.5, 7.0	−	> 3 months
21/4/2016	08:45−08:55	WM−KLY / WM−KLY-1	1.0,2.0,4.0	−	>3 months
2/5/2016	08:45−08:55	TMRX−ET / TMRX−ET-1	4.5, 5.5, 7.5	−	>3 months
3/5/2016	08:45−08:55	WM−KLY / WM−KLY-2	1, 2, 4	−	>3 months
25/5/2016	08:30−08:40	BARE−MSD / BARE−MSD-1	1.25, 2.5, 5	−	1−2
26/5/2016	08:30−08:40	BARE−MSD / BARE−MSD-2	1.25, 2.5, 5	−	2−3
30/5/2016	12:00−12:10	WM−ET / TMRX−ET-2	4.5, 5.5, 7.5	−	>3 months
31/5/2016	12:00−12:10	BARE−MSMR / BARE−MSMR-2	2.5, 4.5, 7	−	>3 months
11/7/2016	12:00−12:20	BARE−MSD / BARE−MSD-3	1.25, 2.5, 5	−	>3 months
11/7/2016	18:00−18:20	BARE−MSD / BARE−MSD-4	1.25, 2.5, 5	−	>3 months
21/2/2017	11:20−11:40	COAST−TKM-SD / COAST−TKM-SD-w	1, 2.5, 6.5	+/−	5
22/2/2017	11:00−11:20	COAST−TKM-LD / COAST−TKM-LD-w	1.5, 3, 7	−	6
28/2/2017	11:20−11:40	COAST−EGD-SD / COAST−EGD-SD-w	1, 2.5, 6.5	+	0
1/3/2017	11:07-11:27	COAST−EGD-MD / COAST−EGD-MD-w	1, 2.5, 6.5	+/−	>3 months
2/3/2017	11:00-11:20	COAST−EGD-LD / COAST−EGD-LD-w	1, 2.5, 6.5	−	>3 months
2/3/2017	12:55-13:15	SEA−KDM / SEA−KDM-w	1	+	>3 months
25/4/2017	11:30-11:50	COAS-EGD-SD / COAST−EGD-SD-s	1, 2.5, 6.5	+	>3 months
26/4/2017	11:00-11:20	COAST−EGD-MD / COAST− EGD-MD-s	1, 2.5, 6.5	+/−	>3 months
27/4/2017	11:00-11:20	COAST−EGD-LD / COAST−EGD-LD-s	1, 2.5, 6.5	−	>3 months
3/5/2017	12:10-12:30	COAST−TKM-SD / COAST−TKM-SD-s	1, 2.5, 6.5	−	>3 months
4/5/2017	10:30-10:50	COAST−TKM-LD / COAST−TKM-LD-s	1.5, 3, 7	−	>3 months
4/5/2017	12:30-12:50	SEA−KDM / SEA−KDM-s	1	+	>3 months

[a] The suffixes "s" and "w" refer to samplings during spring and winter, respectively. "SD", MD", and "LD" refer to relatively short, medium, and long distance from the coastline, respectively (see Sect. 2.1). [b] "+", "−" and "+/−" respectively indicate that the samplings could be, could not be, or may be influenced by emission from the

Atmos. Chem. Phys. Discuss., https://doi.org/10.5194/acp-2018-1172
Manuscript under review for journal Atmos. Chem. Phys.
Discussion started: 17 December 2018

Atmospheric Chemistry and Physics Discussions

236 seawater. [c] Values indicate the number of days before sampling during which precipitation occurred. Additional
237 abbreviations: MSD, Masada; MSMSR, Mishmar; KLY, Kalya; ET, Ein-Tamar; KDM, Kedem; EGD, Ein-Gedi;
238 BARE, bare soil site; COAST, coastal soil-salt mixture site; WM, cultivated watermelon site; TMRX, natural
239 Tamarix site; SEA, sampling near the seawater (see Sect. 2.1.1).
240

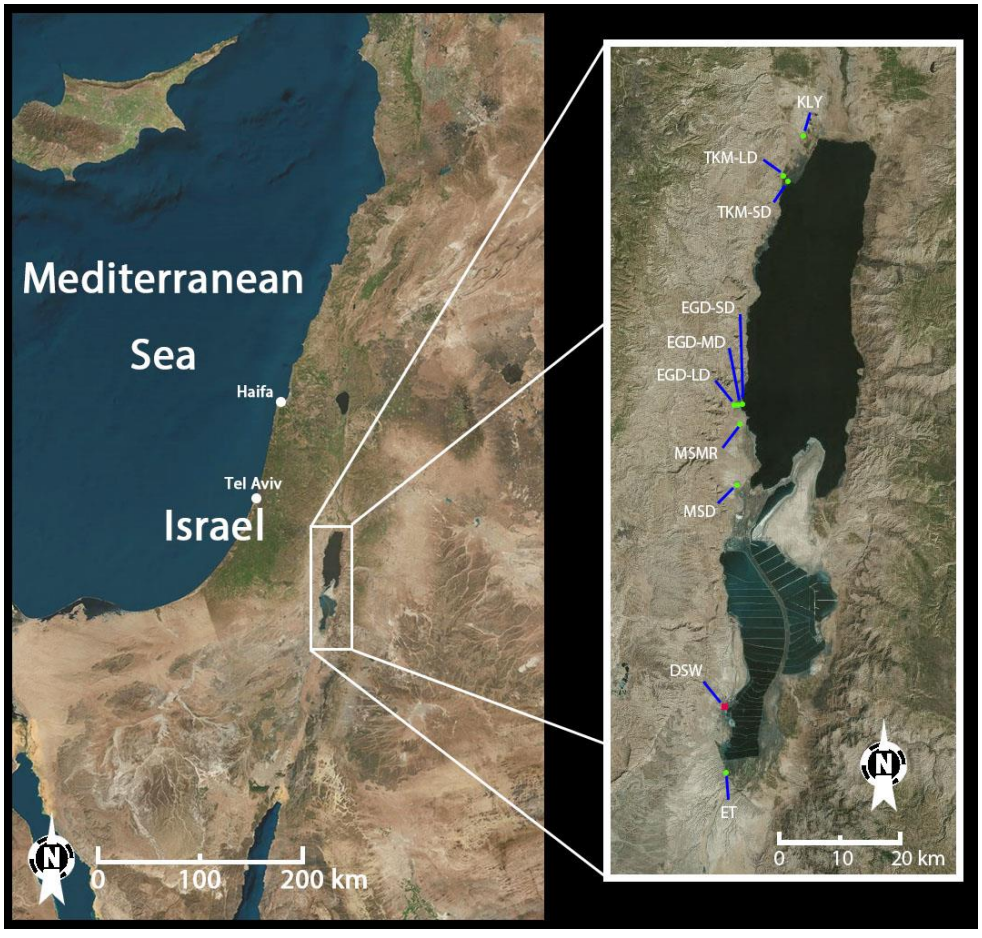

241
242 **Fig. 1**. Location and satellite image of the Dead Sea measurement sites and Dead Sea Works (DSW). Left: location
243 of the Dead Sea. Right: zoom-in of the area of measurement sites.
244

245 **2.2 Vertical flux evaluation**

246 The vertical flux, F_c, of a species c, was evaluated according to the gradient approach using the
247 vertical gradient of c, $\frac{\partial C}{\partial z}$, and a constant, K_c:

Atmos. Chem. Phys. Discuss., https://doi.org/10.5194/acp-2018-1172
Manuscript under review for journal Atmos. Chem. Phys.
Discussion started: 17 December 2018

Atmospheric Chemistry and Physics Discussions

$$F_c \equiv -K_c \frac{\partial C}{\partial z} \quad (1)$$

K_c represents the rate of turbulent exchange in Eq. 1 and was evaluated on the basis of the Monin−Obukhov similarity theory (MOST) described by Lenschow (1995):

$$K_{C(z)} = u_* K Z \phi_C(\zeta) \quad (2)$$

where u_* is the friction velocity, K is the Von Kármán constant, Z is the measurement height and ϕ_C is a universal function of the dimensionless parameter ζ. According to MOST, vertical fluxes in the surface layer can be evaluated on the basis of the dimensionless length parameter, ζ, according to

$$\zeta = (z - d)/L \quad (3)$$

where z, d and L are the vertical coordinate, zero displacement, and the Monin−Obukhov length, respectively (Schmugge and André, 1991).

We relied on the commonly used assumption that ϕ_C is similar to ϕ_h for chemical species with a relatively long lifetime (Dearellano et al., 1995), and calculated ϕ_h using the following equation for the relationship between ϕ_h and ζ, which was found to be valid for 0 .004 ≤– z/L≤ 4 (Dyer and Bradley, 1982;Yang et al., 2001):

$$\phi_h = (1 - 14\zeta)^{-1/2} \quad (4)$$

We derived L from the Pasquill and Gifford stability class (Pasquill and Smith, 1971) and roughness length (z_0) according to Golder D. (1972). $z_0$was evaluated based on the specific surface characteristics at each site using information provided by the WMO (2008). The stability class was evaluated using the in-situ measured solar radiation and wind speed (Gifford, 2000;Pasquill and Smith, 1971). u_* was derived from the logarithmic wind profile according to MOST, using the following equation:

$$u(z) = \frac{u^*}{k}\ln\left(\frac{z-d}{z_0}\right) \quad (5)$$

where u(z) is the wind speed at height z, and ψ_m is a correction for diabatic effect on momentum transport. Using the measured u at a height of 10 m, we calculated the wind speed at each measurement height according to Gualtieri and Secci (2011):

$$u_2 = u_1 \frac{\ln(z_2/z_0) - \psi m(z_2/L)}{\ln(z_1/z_0) - \psi m(z_1/L)} \quad (6)$$

where ψ_m is calculated using:

$$\Psi m(Z/L) = 2\ln(1+X/2) + \ln(1+X^2)/2) - 2\arctan(X) + \pi/2 \quad (7)$$

and

$$X = (1 - 15\left(\frac{z}{L}\right))^{1/4} \quad (8)$$

2.3 Soil analyses

Soil samples at each site were collected up to a depth of 5 cm during summer, at least 3 months following any rain event in the Dead Sea area. The samples were analyzed for bromine, chlorine, iodine, organic matter, moisture and Fe in the soil, as well as for pH of the soil. Prior to halide quantification, extractions for each sample were prepared using HNO_3. Total Br and I were quantified using inductively coupled plasma mass spectrometry (ICPMS). Total Cl was quantified by potentiometric titration against $AgNO_3$.

To quantify Fe in the soil, microwave-assisted digestion with reverse aqua regia was used, and Fe concentration was determined by inductively coupled plasma optical emission spectrometry (ICP−OES). A batch of each sample (~300 mg of dry soil) was digested in reverse aqua regia (HNO_3 (65 %) : HCl (30 %); 3:1 mixture). Digestion was allowed to proceed in quartz vessels using a "Discover" sample digestion system at high temperature and pressure (CEM Corporation, NC, USA). The vessels were cooled and the volume was made up to 20 mL with deionized water. Element concentrations were measured in clear solutions using High Resolution dual-view ICP−OES PlasmaQuant PQ 9000 Elite (Analytik Jena, Germany). The

reported values represent a low−limit, because the samples were not completely dissolved. Soil water content and organic matter (OM) were determined by weight loss under dry combustion at 105 °C and 400 °C, respectively. Soil pH was measured in 1:1 soil-to-water extracts with a model 420 pH-meter (Thermo Orion, Waltham, MA, USA).

3 Results and discussion

3.1 VHOC flux and mixing ratio

We compared the measured mixing ratios and fluxes with corresponding available information. Overall, measurements at the Dead Sea boundary layer revealed that the mixing ratios for all investigated VHOCs were higher than their background MBL levels, pointing to significant local emissions. No association was observed between the measured mixing ratios and the air masses flowing from the direction of the Dead Sea Works, which is located to the north-west of the TMRX−ET site and to the south of all other measurement sites (see Fig. 1), and is the main anthropogenic source in the area under investigation. The absence of any such association points to the dominance of natural sources for the VHOCs in the studied area. Table 2 presents a comparison between measured mixing ratios at the different measurement sites and reported values for the global MBL. The values indicate that median mixing ratios at the Dead Sea are higher than corresponding mixing ratios in the MBL by factors of 1.2−8.0 for brominated and chlorinated VSLS and ~1.5, 1.3 and 1.1 for CH_3I, CH_3Br and CH_3Cl, respectively. Moreover, as described below, measured mixing ratios at the Dead Sea were generally also higher than in coastal areas.

Owing to their large contribution to stratospheric bromine, $CHBr_3$ and CH_2Br_2 are the most extensively studied VSLS in the MBL (Hossaini et al., 2010). The mixing ratios of $CHBr_3$ and CH_2Br_2 that we measured at the Dead Sea ranged from 1.9 to 22.6 pptv and from 0.7 to 18.6 pptv, respectively, which are higher than most of their reported mixing ratios in coastal areas

Atmos. Chem. Phys. Discuss., https://doi.org/10.5194/acp-2018-1172
Manuscript under review for journal Atmos. Chem. Phys.
Discussion started: 17 December 2018

where the highest mixing ratios have typically been measured. For example, Carpenter et al. (2009) reported elevated mixing ratios for $CHBr_3$ and CH_2Br_2 along the eastern Atlantic coast ranging from 1.9 to 4.9 and from 0.9 to 1.4 ppt, respectively, and Nadzir et al. (2014) reported mixing ratios of 0.82−5.25 pptv and 0.90−1.92 ppt for $CHBr_3$ and CH_2Br_2, respectively, for several tropical coastal areas including the Strait of Malacca, the South China Sea and Sulu-Sulawesi Seas. Somewhat higher mixing ratios for $CHBr_3$ have been measured in only a few locations, including some at coastal areas near New Hampshire (Zhou et al., 2008), San Cristobal Island (Yokouchi et al., 2005;O'Brien et al., 2009), Cape Verde (O'Brien et al., 2009), Borneo (Pyle et al., 2011) and Cape Point (Kuyper et al., 2018;Butler et al., 2007), where the range (and average) concentrations at those locations were 0.2−37.9 pptv (5.6−6.3), 4.2−43.6 pptv (14.2), 2.0−43.7 pptv (4.3−13.5), 2−60pptv (−) and 4.4−64.6 pptv (24.8), respectively. For CH_2Br_2, the corresponding mixing ratios were reported as 1.3–2.3 pptv, 0.5−4.1 pptv and 0.7−8.8 pptv in New Hampshire, San Cristobal Island and Cape Verde, respectively, which are comparable with the mixing ratios measured at the Dead Sea.

Figure 2 presents the measured fluxes of all VHOCs studied. On average, the net fluxes of all measured species, except C_2HCl_3 and CH_3I, were positive at most of the investigated sites. The flux magnitudes for $CHBr_3$ and CH_2Br_2 were higher than for most reported emissions at the MBL, but in most cases were smaller than the corresponding average fluxes estimated by Butler et al. (2007) for global coastal areas (~220 and 110 nmol m^{-2} d^{-1}), respectively. In some cases, however, the fluxes of both species were higher than these values.

$CHCl_3$ emission rates were positive for most measurements and particularly high for TMRX−ET-2 (213 nmol m^{-2} d^{-1}), COAST−EGD-SD-s (883 nmol m^{-2} d^{-1}), and BARE−MSMR-1 (247 nmol m^{-2} d^{-1}) (see Yi et al., 2018). For comparison, the emission from BARE−MSMR-1 is similar to the maximum emission found for tundra peat by Rhew et al. (2008), while the averaged emissions from COAST−EGD-SD-s and TMRX−ET-2 are higher than those from temperate peatlands (~496 nmol m^{-2} d^{-1} as measured by Dimmer et al. (2001)).

Atmos. Chem. Phys. Discuss., https://doi.org/10.5194/acp-2018-1172
Manuscript under review for journal Atmos. Chem. Phys.
Discussion started: 17 December 2018

346 Whereas emissions during COAST−EGD-SD-s and TMRX−ET-2 might have been affected by
347 vegetation and seawater, respectively, the emission from BARE−MSMR can be completely
348 attributed to soil. The latter emission flux in BARE−MSMR is higher than the maximum
349 emission rate in arctic and subarctic soils (~115 nmol m^{-2} d^{-1}) reported by Albers et al. (2017).

350 Average calculated fluxes for the additional brominated VSLS, $CHBr_2Cl$, and $CHBrCl_2$
351 were positive for all sites except for $CHBr_2Cl$ at COAST−TKM. The mixing ratios of $CHBr_2Cl$
352 and $CHBrCl_2$ were higher by factors of ~4−14 and ~5−11, respectively, than the average
353 reported values for the MBL and were also higher than measured mixing ratios in nearby coastal
354 areas, except for the extremely high $CHBr_2Cl$ mixing ratios emitted from a rock pool at Gran
355 Canaria (ranging from 19 to 130 ppt; (Ekdahl et al., 1998)). For example, Brinckmann et al.
356 (2012) found mean mixing ratios for $CHBr_2Cl$ and $CHBrCl_2$ in coastal areas at the Sylt Islands
357 (North Sea) of up to 0.2 and 0.1 ppt, respectively, while Nadzir et al. (2014) found $CHBr_2Cl$ and
358 $CHBrCl_2$ mixing ratios of 0.07–0.15 ppt and 0.15–0.22 ppt, respectively, in the tropics. The
359 measured fluxes that we obtained for $CHBr_2Cl$ at the Dead Sea are also higher than the reported
360 values of 0.8 (range, -1.2−10.8) nmol $m^{-2}d^{-1}$ at coastal areas sampled during the Gulf of
361 Mexico and East Coast Carbon cruise (GOMECC), (Liu et al., 2011). Typically, the $CHBrCl_2$
362 net flux at the Dead Sea is significantly higher than corresponding fluxes from arctic and
363 subarctic soils, as recently reported by Albers et al. (2017) (see Fig. 2).

364 The CH_3Cl flux at the Dead Sea was positive for only half of the measurements, while a net
365 positive flux for all measurements was obtained only at COAST−TKM. The highest positive
366 fluxes were measured at COAST−EGD and COAST−TKM, with maximum net fluxes of
367 ~10800 and 4900 nmol m^{-2} d^{-1}, respectively. These fluxes are comparable in magnitude to those
368 reported for several terrestrial sources, such as tropical forests (~4520 nmol m^{-2} d^{-1}) by
369 Gebhardt et al. (2008) or by Yokouchi et al. (2002) and for other tropical or subtropical
370 vegetation (Yokouchi et al., 2007), and they are higher than emissions from dryland ecosystems
371 including shortgrass steppe or shrublands (Rhew et al., 2001). In some cases the measured

fluxes were higher than average emissions from salt marshes (e.g., ~7300 nmol m^{-2} d^{-1}; (Deventer et al., 2018)), but significantly smaller than the maximum fluxes (e.g., 570000 nmol m^{-2} d^{-1}; (Rhew et al., 2000)).

In contrast to CH_3Cl, emissions of CH_3Br at the Dead Sea were significantly lower than the average reported emissions from marshes (e.g., ~600 nmol m^{-2} d^{-1}; (Deventer et al., 2018). The fluxes measured at the Dead Sea were also lower than the reported emission from a coastal beach in a Japanese archipelago island (~53000 nmol m^{-2} d^{-1}), but higher, in most cases, than in other dryland ecosystems (see Rhew et al. (2001)).

The net flux of CH_3I measured at the Dead Sea was negative in 60 % of the measurements. Positive measured net fluxes of this compound were in most cases comparable to other reported fluxes over soil and vegetation. For example, Sive et al. (2007) reported a CH_3I flux of ~18.7 nmol m^{-2} d^{-1} over soil and vegetation at the AIRMAP Observing Station at Thompson Farm, NH, USA, and a somewhat lower emission (~12.6 nmol m^{-2} d^{-1}) at Duke Forest, NC, USA. While the elevated flux during COAST−EGD-SD-s (17.0 nmol m^{-2} d^{-1}) could potentially have been affected by flow of the sampled air over the seawater, the positive net fluxes in BARE−MSMR (1.00 and 4.42 nmol m^{-2} d^{-1}) indicate significant emission from bare soil at the Dead Sea. The emission rates in BARE−MSMR are similar to the measured soil-emission fluxes of CH_3I reported by Sive et al. (2007) at Duke Forest, averaging ~0.27 nmol m^{-2} d^{-1} (range, ~ 0.11−4.1 nmol m^{-2} d^{-1}).

Most of the sites were found, on average, to be a sink for C_2HCl_3, which may suggest that the elevated mixing ratios for this species in the Dead Sea area mostly result from anthropogenic emission.

Atmos. Chem. Phys. Discuss., https://doi.org/10.5194/acp-2018-1172
Manuscript under review for journal Atmos. Chem. Phys.
Discussion started: 17 December 2018

Atmospheric Chemistry and Physics Discussions

394 **Table 2**. Comparison of VSLS and methyl halide mixing ratios (in pptv) measured at the Dead Sea with their
395 corresponding values at the marine boundary layer (MBL). Unless otherwise specified, the table presents median,
396 minimum and maximum VHOC mixing ratios measured at different sites at the Dead Sea (see Table 1 for site
397 abbreviations) and in the MBL, as reported by Carpenter and Reimann et al. (2014).

Species	Median/ Range	BARE−MSMR	BARE−MSD	COAST−EGD	COAST−TKM	TMRX−ET	WM−KLY	SEA−KDM	All Sites	EF. MBL[a]
$CHBr_3$	Median	11.3	11.0	8.0	2.6	4.7	3.1	11.0	**6.2**	**5.2**
	Range	5.6−16.3	6.0−22.6	4.4−16.8	3.6−1.9	2.9−7.1	2.3−3. 5	5.4−16.5	**1.9−22.6**	**4.8–5.7**
CH_2Br_2	Median	0.9	2.7	1.8	0.8	1.3	1.1	1.4	**1.1**	**1.22**
	Range	0.9−1.0	0.7−18.6	0.9−5.1	0.9−0.8	0.9−1.6	1.0−1.2	1.1−1.7	**0.7−18.6**	**1.2–11**
$CHBr_2Cl$	Median	4.8	4.1	2.2	1.2	2.2	0.9	1.3	**2.4**	**8**
	Range	3.2 −5.4	2.2−11.0	0.4−6.5	7.5−0.5	0.6−3.6	0.5−1.0	0.5−2.2	**0.4−11.0**	**4–14**
$CHBrCl_2$	Median	2.6	2.5	1.6	1.0	2.4	0.9	2.0	**1.4**	**4.7**
	Range	2.6−3.7	0.9−9.6	1.0−3.0	0.5−1.4	0.7−3.9	0.6−1.1	1.3−2.7	**0.5−9.6**	**5–11**
C_2HCl_3	Median	1.15	1.7	1.3	1.6	1.1	2.7	1.2	**1.5**	**3**
	Range	1.22-0.84	1.0−2.7	0.3−10.5	0.4−2.9	0.4−1.5	1.0−4.1	0.8−1.6	**0.4−10.5**	**8–5.3**
$CHCl_3$	Median	16.9	19.8	18.2	18.7	19.0	19.8	17.3	**18.63**	**2.5**
	Range	15.9−20. 5	18.8−25.3	14.5−27.9	15.4−20.1	18.4−57.2	18.8−5.3	16.5−18.2	**14.5−57.2**	**2.0–7.3**
CH_3I	Median	0.8	1.3	1.2	1.5	1.3	1.1	1.4	**1.2**	**1.5**
	Range	0.8−0.8	1.0−1.5	0.4−2.1	1.5−1.2	0.8−2.8	0.7−1.6	1.2−1.6	**0.4−2.8**	**1.3– 1.3**
CH_3Br	Median	8.72	10.3	8.7	8.4	10.0	8.4	9.7	**9.1**	**1.3** [b]
	Range	8.1−9.4	7.8−13.8	7.5−13.3	8.5−7.5	8.3−13.8	7.8−9.2	9.1−10.2	**7.5−13.8**	**N/A**
CH_3Cl	Median	596	571	595	580	623*	643	596	**601**	**1.1 b**
	Range	583−608	549−672	531−732	583−545	581−685*	591−668	583−608	**531−732***	**N/A**

398

399 [a] Values represent the enrichment factor (EF) at the Dead Sea, reflected as the ratio between the median measured
400 mixing ratios and the corresponding median values for the MBL; [b]EF is calculated using the annual average for
401 2012 based on flask measurements by the US National Oceanic and Atmospheric Administration (NOAA)
402 (http://www.esrl.noaa.gov/gmd/dv/site/ and in-situ measurements by the Advanced Global Atmospheric Gases
403 Experiment (AGAGE (http://agage.eas.gatech.edu/). See Table 1 for site abbreviations. *Calculation excludes one
404 CH_3Cl measurement in TMRX−ET-1 (see Sect. 2.1.2).

Atmos. Chem. Phys. Discuss., https://doi.org/10.5194/acp-2018-1172
Manuscript under review for journal Atmos. Chem. Phys.
Discussion started: 17 December 2018

Atmospheric Chemistry and Physics Discussions

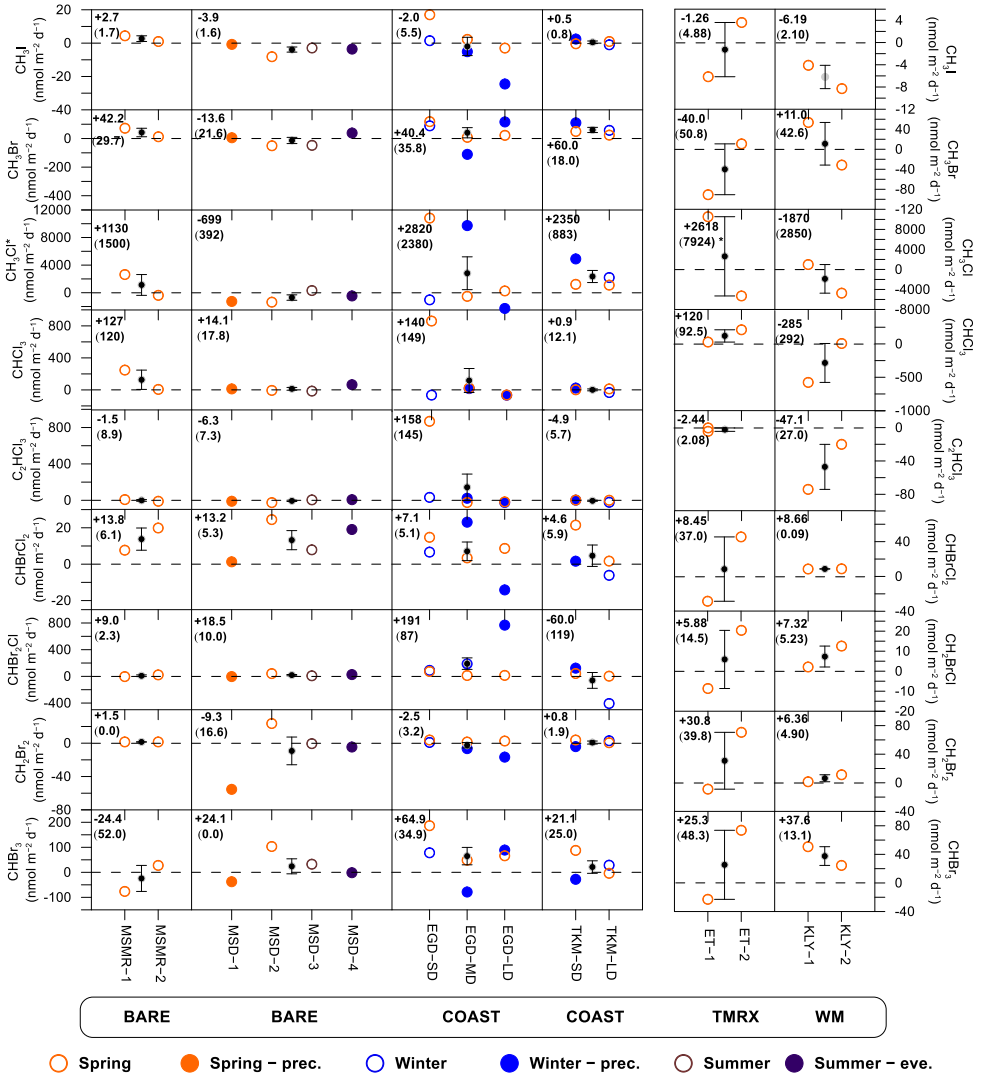

Fig. 2. VHOCs fluxes at the different measurement sites. Fluxes are marked by circles to individually indicate measurements during spring, winter, summer, up to 3 days after a rain event in spring ("Spring-prec."), up to 6 days after a rain event in winter ("Winter-prec.") and in summer during evening ("Summer-eve"); for more information about measurement conditions see Table 1. Black filled circles and error bars respectively represent the average and standard error of the mean (SEM) for each measurement site. Dashed lines represent zero flux. Mean flux value and standard deviation (SD; in parenthesis) are shown for each site and species. See Table 1 for measurement sites and measurement abbreviations. * Calculation of mean flux and SD excludes one CH_3Cl measurement in TMRX−ET-1 (see Sect. 2.1.2).

Atmos. Chem. Phys. Discuss., https://doi.org/10.5194/acp-2018-1172
Manuscript under review for journal Atmos. Chem. Phys.
Discussion started: 17 December 2018

414 **3.2 Factors controlling the flux of VHOCs**

415 **3.2.1 Seasonal, meteorological and spatial effects**

416 The results presented in Sect. 3.1 record elevated mixing ratios and net fluxes for all
417 investigated VHOCs, with relatively less frequent positive fluxes for CH_3I and C_2HCl_3. All of
418 the investigated VHOCs except C_2HCl_3 were associated with a positive average net flux from at
419 least one of the two bare soil sites BARE−MSMR and BARE−MSD (Fig. 2), and for all
420 VOHCs, except C_2HCl_3 and CH_3Cl, all measured mixing ratios were highest over at least one of
421 these bare soil sites (Table 2). These findings suggest that a significant emission for all of the
422 investigated VHOCs occurred from bare soil located within at least a few kilometers from the
423 Dead Sea water.

424 No clear impact of meteorological conditions on the measured net flux rates or mixing ratios
425 was observed. We could not identify any clear association between flux magnitude and any
426 parameter, including solar radiation intensity, measurement time, temperature, or daytime
427 relative humidity.

428 Our findings on the effects of season and distance from the sea on the measured fluxes are
429 presented in Fig. 2, which presents the results of our measured fluxes for spring and winter and
430 for different distances from the sea at COAST−EGD and COAST−TKM. It can be seen from the
431 figure that whereas for most compounds there were no clear differences in fluxes between
432 spring and winter, the measured fluxes for CH_3I, $CHBrCl_2$ and CH_2Br_2 were generally higher in
433 the spring. No clear impact of the distance from the seawater on the measured net fluxes could
434 be detected, including in cases where a significant fraction of the footprint included the
435 seawater, such as during COAST−TKM-SD-w and, to a lesser extent, during COAST−EGD-
436 SD-w and COAST−EGD-SD-s. However, as discussed below (see Sects. 3.2.2, 3.2.3), owing to
437 variations in soil properties the emissions near the seawater tended to be more frequent and
438 more intense. Figure 3 compares the mixing ratios of the measured VHOCs at different
439 distances from the seawater, and individually for winter and spring. No clear impact of season

Atmos. Chem. Phys. Discuss., https://doi.org/10.5194/acp-2018-1172
Manuscript under review for journal Atmos. Chem. Phys.
Discussion started: 17 December 2018

Atmospheric Chemistry and Physics Discussions

or distance from the seawater on the mixing ratios can be discerned in this figure, also for the sampling over SEA−KDM which directly represented air masses over the seawater (Sect. 2.1.1). Nevertheless, further investigation, using direct flux measurements over the Dead Sea water, is needed to study the potential emission of VHOCs from the Dead Sea water.

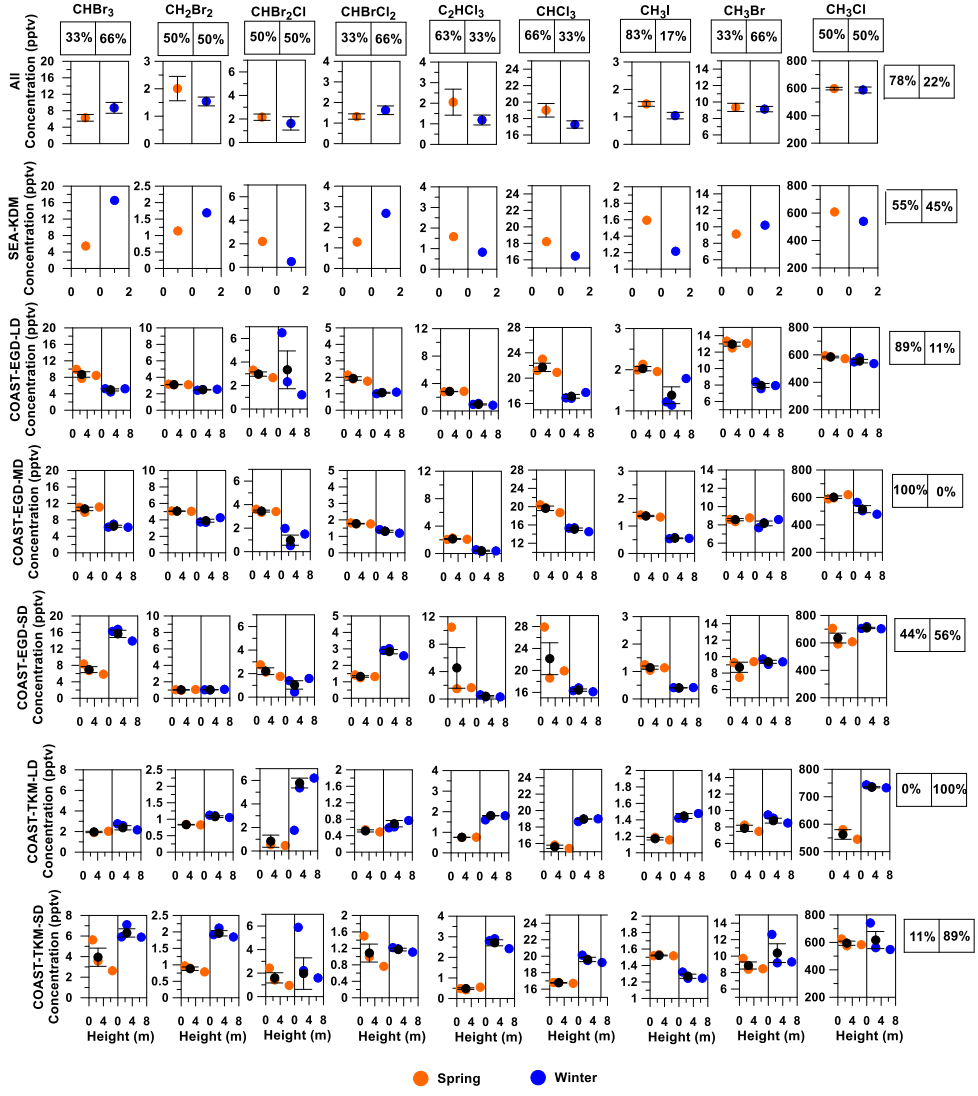

Figure 3. Seasonal and spatial influences on measured mixing ratios of VHOCs. Measured VHOC mixing ratios are presented vs. vertical height above surface level, separately for winter (blue) and spring (orange). Black filled circles and error bars represent the average and SEM, respectively. Values above and to the right of the figure indicate the percentage of time during which average mixing ratios were higher during spring (left box) or

448 during winter (right box), individually for TKM, EGD and SEA−KDM sites, and for all of these sites together
449 (All), for all sites and all species, respectively (see Table 1 for measurement site abbreviations).
450

451 **3.2.2 Impact of specific site characteristics and ambient conditions**

452 The formation of VHOCs requires a chemical interaction between organic matter and halides,
453 induced by biogeochemical, biochemical, or macrobiotic processes (Kotte et al., 2012;Breider
454 and Albers, 2015). Despite the extreme salinity, biotic activity was detected both in the water
455 and in the soil of the Dead Sea (see Sect. 1), demonstrating that biotic activity can potentially
456 contribute to VHOC emission in this area. Previous studies on emission of VHOCs from soil
457 and sediments revealed that organic matter content and type, halide ion concentrations, pH, and
458 the presence of an oxidizing agent (most frequently referred to Fe (III)) also play important roles
459 in the emission rate of VHOCs (see (Kotte et al., 2012)).

460 Table 3 provides a basic representation of these parameters. The table records substantial
461 enrichment of Cl and Br in the sites closest to the seawater (COAST−EGD-SD and
462 COAST−TKM-SD) and lower concentrations at larger distance from the seawater. For
463 comparison, both Br and Cl concentrations are much higher than those reported by Kotte et al.
464 (2012) for various saline soils and sediments (0.12−0.32 g kg^{-1} and 6.1−120 g kg^{-1},
465 respectively), but are lower in BARE−MSMR and BARE−MSD for Br and for both Cl and Br
466 in WM−KLY. No enrichment of I in the soil samples was observed (e.g., see Keppler et al.
467 (2000);Kotte et al. (2012)). The OM content of the samples is generally higher than would be
468 expected in desert soil. For comparison, forest floors typically contain 1−5 % OM (Osman,
469 2013). Detection of VHOC emissions from the soil was in some cases associated with higher
470 soil OM (e.g., Albers et al., 2017; Kepller et al., 2000) and in some cases with lower soil OM
471 (e.g., Kotte et al., 2012; Hubber et al., 2009) than reported here. Table 3 provides only an
472 underestimated value of Fe, rather than Fe (III), in the samples. Note, however, that similar soil
473 Fe content as reported here as a low-limit value corresponded with the finding of small amounts
474 of VHOCs emission, while the emission rates became saturated when enrichment with Fe (III)

was relatively minor (Keppler et al., 2000). Saturation at relatively low soil Fe concentrations was also reported by Huber et al. (2009). Hence, variations in Fe across different sites may result in different emission rates.

Table 4 merges the mixing ratios, fluxes, and the ratio between flux and corresponding mixing ratio (F:C) during all measurement periods, for all investigated VHOCs. F:C is used to study the potential contribution of each site to the VHOC mixing ratios measured at that site. The number of samplings at each site was limited, but Table 4 indicates that the fluxes measured at some of the sites were relatively high. In both COAST−TKM and COAST−EGD sites we observed relatively high frequencies of elevated fluxes, particularly from the SD sites, and to some extent also in COAST−EGD-MD. Moreover, for both COAST−EGD and COAST−TKM, during both spring and winter the occurrence of positive fluxes was correlated with proximity to seawater (i.e., COAST−EGD-SD > COAST−EGD-MD > COAST−EGD-LD, and COAST−TKM-SD > COAST−TKM-LD). All of these sites contain mixtures of soil and salt-deposited structures (see Sect. 2.1.1), and Table 3 indicates that soil concentrations of both Br and Cl correlated with proximity to seawater at both COAST−EGD and COAST−TKM. The concentration of I in the soil showed a similar trend only in COAST−TKM (see Table 3). This association between the positive net flux magnitude and incidence and the soil halide concentrations points to an increase in VHOC emission with salinity, even under the hypersaline conditions of the Dead Sea area. This interpretation is supported by the fact that whereas for COAST−TKM-SD both soil water and OM content were relatively high, for COAST−EGD-SD no other parameter, except for the halides soil concentration, was clearly higher for COAST−EGD-MD and COAST−EGD-LD. The generally higher emission rates for COAST−EGD than for COAST−TKM (Table 4) may suggest, in view of the apparently lower Fe content for COAST−EGD (Table 3), that the emission of VHOCs from these sites was not significantly limited by the availability of Fe (III) in the soil.

Atmos. Chem. Phys. Discuss., https://doi.org/10.5194/acp-2018-1172
Manuscript under review for journal Atmos. Chem. Phys.
Discussion started: 17 December 2018

Our measurements revealed no clear contribution of vegetation to the emission fluxes or the mixing ratios (Fig. 2 and Table 2), but it should be emphasized that our ability to define their role in VHOC emission and uptake in this study was limited. Table 4 indicates relatively high positive net fluxes for several species in one out of the two measurements at each of the vegetated sites TMRX−ET and WM−KLY. Particularly for TMRX−ET-2, emissions were high for all of the investigated VSLS except C_2HCl_3 and CH_3Cl (Fig. 2, Table 4).

Whereas during COAST−EGD-SD-s all measured emission fluxes were positive and high, emissions during COAST−EGD-SD-w were generally lower and were negative for CH_3Cl and $CHCl_3$. Based on the wind direction, in both cases the sampling footprint included both the seawater and a narrow strip of bare soil mixed with salty beds (estimated at about 40 % of the footprint), very close to the seawater. The main notable difference between the two measurement days is that precipitation occurred just before COAST−EGD-SD-w, while there was no precipitation event for several weeks prior to COAST−EGD-SD-s. Note that the much higher fluxes during COAST−EGD-SD-s than during COAST−EGD-SD-w did not result in a proportional increase in F:C (e.g., for C_2HCl_3), and for some species the F:C for COAST−EGD-SD-s was even lower than for COAST−EGD-SD-w (e.g., for $CHBr_3$ and CH_3Br). This decoupling between fluxes and mixing ratios may be attributable to the fact that flux and concentrations can have very different footprints, such that under a widespread rain event the mixing ratios at COAST−EGD-SD might be less directly affected by the local changes in the net fluxes.

A less widespread and more spatially limited rain event occurred ~1.5 and ~2.5 days before BARE−MSD-1 and BARE−MSD-2, respectively. It is notable that the emission fluxes for BARE−MSD-1 are lower and more negative for most of the species than those for BARE−MSD-3 or BARE−MSD-4. Also, the occurrence of positive net flux increased according to the order BARE−MSD-1 < BARE−MSD-2 < BARE−MSD-3 < BARE−MSD-4 (see Table 4). This suggests that increased soil water content caused by rain events can decrease the emission

Atmos. Chem. Phys. Discuss., https://doi.org/10.5194/acp-2018-1172
Manuscript under review for journal Atmos. Chem. Phys.
Discussion started: 17 December 2018

rates of certain VHOCs. Furthermore, the local rain event in BARE−MSD may be a major reason for the generally more frequent and higher net fluxes in BARE−MSMR than in BARE−MSD, and the fact that unlike in the case of COAST−EGD-SD measurements, the low flux values for BARE−MSD-1 are accompanied, in most cases, by proportionally low F:C values (Table 4). Interestingly, ~2.5 days after the rain event the measured fluxes at BARE−MSD-2 were higher for all brominated VSLS but negative for all other VHOCs, which may indicate the involvement of microbial activity in the emission processes.

The reduction in net flux rates following rain events did not occur for all species, and there was no clear consistency in this aspect across the two sites BARE−MSD and COAST−EGD-SD. Thus, further research on the effects of rain on the various VHOCs and ambient conditions is required. Nevertheless, the analyses clearly demonstrate that strong emission rates do not depend on rain occurrence, in agreement with findings by Kotte et al. (2012). The lower emission fluxes following the rain event may be attributable to the low infiltration rate of VHOCs through the soil, or by salt dilution and washout, or both.

Table 3. Soil properties. OM, organic matter; soil water content (SWC); I, Br, Cl and Fe dry weight fraction and soil pH. See Table 1 for measurement site abbreviations.

Site	pH	OM (%)	SWC (%)	I mg kg soil dw^{-1}	Br gr kg soil dw^{-1}	Cl gr kg soil dw^{-1}	Fe mg kg^{-1}
BARE−MSMR	7.46	1.96	1.90	2.24	0.007	6.70	>20800
BARE−MSD	7.41	3.61	3.61	2.79	0.027	41.2	>7450
COAST−EGD-SD	7.61	2.28	1.79	0.24	1.47	202	>1120
COAST−EGD-MD	7.93	0.35	0.35	0.57	0.293	37.4	>3140
COAST−EGD-LD	7.70	3.67	2.58	1.03	0.008	26.1	>5950
COAST−TKM-SD	7.43	24.1	33.7	3.19	3.93	169	>12500
COAST−TKM-LD	7.80	3.40	1.64	1.14	0.186	19.5	>10600
TMRX−ET	7.88	3.14	2.97	2.69	0.474	85.2	>10100
WM−KLY	7.64	4.10	1.40	1.69	0.013	1.12	>7680

Atmos. Chem. Phys. Discuss., https://doi.org/10.5194/acp-2018-1172
Manuscript under review for journal Atmos. Chem. Phys.
Discussion started: 17 December 2018

Atmospheric Chemistry and Physics Discussions

544 **Table 4.** VHOC flux and its correspondence with mixing ratios. Shown are the measured flux (nmol m^{-2} d^{-1}, upper
545 cells; bold) and the ratio between flux and mixing ratio (ppt; F:C; lower cells; italic), obtained for the different
546 measurements. Also shown are the average flux ("Mean") and average positive flux ("Mean positive") for all
547 species, as well as the incidence of positive flux (*X*) individually for each site and each VHOC. (See Table 1 for
548 abbreviations of the different measurements).

549

Species / Site	CH_2Br_2	$CHBr_3$	$CHBr_2Cl$	$CHBrCl_2$	$CHCl_3$	C_2HCl_3	CH_3Cl	CH_3Br	CH_3I	*X* (%)
BARE–MSMR-1	**1.43**	**-76.5**	**-3.27**	**7.68**	**247**	**7.33**	**2629**	**71.9**	**4.42**	**77.8**
	1.59	*-4.84*	*-0.62*	*2.94*	*13.3*	*6.36*	*4.03*	*8.22*	*5.77*	
BARE–MSMR-2	**1.51**	**27.6**	**21.3**	**19.9**	**6.51**	**-10.4**	**-378**	**12.6**	**1.00**	**77. 8**
	1.66	*4.18*	*5.65*	*6.30*	*0.40*	*-9.83*	*-0.69*	*1.47*	*1.29*	
BARE–MSD-1	**-55.4**	**-37.7**	**-3.58**	**1.32**	**12.1**	**-11.0**	**-1266**	**5.26**	**-0.73**	**33.3**
	-3.30	*-4.80*	*-1.61*	*1.38*	*0.61*	*-9.00*	*-2.10*	*0.38*	*-0.55*	
BARE–MSD-2	**23.5**	**103**	**41.8**	**24.5**	**-6.02**	**-24.8**	**-1368**	**-50.3**	**-8.14**	**44.4**
	4.89	*4.95*	*4.01*	*2.66*	*-0.21*	*-10.38*	*-2.14*	*-4.59*	*-7.69*	
BARE–MSD-3	**-0.60**	**32**	**8.69**	**7.92**	**-14.6**	**4.32**	**311**	**-47.9**	**-2.95**	**55. 6**
	-0.82	*5.46*	*2.62*	*3.42*	*-0.96*	*2.38*	*0.56*	*-5.34*	*-2.27*	
BARE–MSD-4	**-4.61**	**-1.41**	**26.96**	**19.1**	**64.7**	**6.39**	**-472**	**38.44**	**-3.58**	**55. 6**
	-5.26	*-0.10*	*5.74*	*7.00*	*3.98*	*3.85*	*-0.85*	*4.37*	*-2.38*	
COAST–EGD-SD-w	**0.85**	**78.1**	**90.0**	**6.63**	**-42.8**	**47.3**	**-1040**	**88.4**	**1.45**	**77. 8**
	0.05	*75*	*78.9*	*5.02*	*-2.61*	*118*	*-1001*	*85.2*	*1.40*	
COAST–EGD-MD-w	**-6.53**	**-79.0**	**187**	**23.1**	**38.5**	**37.5**	**9719**	**-111**	**-5.16**	**55. 6**
	-6.70	*-12.25*	*141*	*17.63*	*3.08*	*92.0*	*17.3*	*-13.6*	*-9.32*	
COAST–EGD-LD-w	**-16.7**	**88.7**	**768**	**-14.2**	**-43.7**	**-8.97**	**-2281**	**116**	**-24.5**	**33.3**
	-6.72	*17.98*	*230*	*-13.40*	*-2.55*	*-9.41*	*-3.83*	*14.6*	*-17.8*	
COAST–EGD-SD-S	**3.71**	**187**	**72.3**	**14.8**	**883**	**884**	**10817**	**118**	**17.0**	**100**
	3.63	*26.80*	*32.9*	*11.21*	*39.9*	*195*	*17.0*	*13.6*	*14.9*	
COAST–EGD-MD-s	**1.35**	**48.6**	**13.4**	**3.42**	**46.4**	**-8.39**	**-530**	**8.10**	**2.27**	**77. 8**
	0.27	*4.54*	*3.88*	*1.93*	*2.36*	*-3.95*	*-0.88*	*0.95*	*1.66*	
COAST–EGD-LD-s	**2.52**	**66.0**	**13.8**	**8.68**	**-40.8**	**-2.03**	**261**	**22.3**	**-2.96**	**66. 7**
	0.81	*7.60*	*4.65*	*4.50*	*-1.90*	*-0.72*	*0.45*	*1.72*	*-1.46*	
COAST–TKM-SD-w	**-4.15**	**-28.1**	**123**	**1.62**	**22.8**	**0.89**	**4895**	**110**	**2.42**	**77. 8**
	-2.12	*-4.46*	*38.1*	*1.38*	*1.16*	*0.33*	*7.56*	*10.6*	*1.91*	
COAST–TKM-LD-w	**2.95**	**28.5**	**-408**	**-6.2**	**-32.9**	**-22.0**	**2200**	**57.3**	**-1.03**	**44.4**
	2.70	*11.4*	*-91.7*	*-9.33*	*-1.75*	*-12.67*	*3.47*	*6.37*	*-0.72*	
COAST–TKM-SD-s	**3.80**	**87.7**	**42.7**	**21.4**	**0.99**	**2.00**	**1210**	**49.3**	**-0.38**	**88. 9**
	4.31	*22.26*	*26.7*	*19.63*	*0.06*	*4.14*	*2.04*	*5.57*	*-0.25*	
COAST–TKM-LD-s	**0.56**	**-3.83**	**2.07**	**1.67**	**12.6**	**-0.31**	**1100**	**23.6**	**0.97**	**77. 8**
	0.68	*-1.95*	*4.14*	*3.21*	*0.81*	*-0.42*	*1.96*	*3.01*	*0.83*	
TMRX–ET-1	**-8.93**	**-23.0**	**-8.64**	**-28.5**	**27.6**	**-0.36**	**10500***	**-90.8**	**-6.14**	**11. 1**
	--6.27	*-7.06*	*-11.5*	*-0.30*	*0.87*	*-0.57*	*12.0*	*-8.46*	*-2.74*	
TMRX–ET-2	**70.6**	**73.7**	**20.4**	**45.4**	**213**	**-4.53**	**-5300**	**10.9**	**3.61**	**77. 8**
	62.5	*11.4*	*5.86*	*12.9*	*11.1*	*-3.23*	*-8.75*	*1.11*	*4.17*	
WM–KLY-1	**1.45**	**50.7**	**2.09**	**8.57**	**-577**	**-74.1**	**983**	**53.5**	**-4.01**	**55. 6**
	1.36	*15.3*	*2.03*	*7.65*	*-27.4*	*-53.1*	*1.53*	*6.30*	*-5.79*	
WM–KLY-2	**11.3**	**24.5**	**12.6**	**8.76**	**6.31**	**-20.0**	**-4730**	**-31.6**	**-8.29**	**66. 7**
	10.9	*8.84*	*19.7*	*13.27*	*0.31*	*-5.44*	*-7.62*	*-3.77*	*-1.36*	
Mean	**1.43**	**32.3**	**51.1**	**8.78**	**41.2**	**40.1**	**1360**	**22.7**	**-1.74**	
	3.84	**9.01**	**25.0**	**4.95**	**2.03**	**15.2**	**-48.0**	**6.39**	**-1.02**	
Mean positive	**9.66**	**68.9**	**90.4**	**13.2**	**122**	**124**	**4060**	**52.4**	**4.14**	
	7.26	**16.6**	**37.9**	**7.18**	**6.00**	**52.8**	**6.17**	**10.9**	**4.00**	
***X* (%)**	**65**	**65**	**80**	**85**	**65**	**40**	**55**	**75**	**40**	

550 * Calculation of flux excludes one CH_3Cl measurement in TMRX–ET-1 (see Sect. 2.1.2).

Atmos. Chem. Phys. Discuss., https://doi.org/10.5194/acp-2018-1172
Manuscript under review for journal Atmos. Chem. Phys.
Discussion started: 17 December 2018

551 **3.2.3 Factors controlling the flux of specific VHOCs**

552

553 Trihalomethanes: Table 4 indicates a higher overall incidence of positive flux measured in
554 brominated than in chlorinated VHOCs, except for $CHCl_3$ for which the net flux is positive for
555 65 % of the measurements. The net flux of the brominated trihalomethanes also tends to be
556 higher than the more chlorinated trihalomethanes ($CHBr_2Cl$ > $CHBr_3$ > $CHBrCl_2$ > $CHCl_3$; see
557 Table 4). When averaging over the positive fluxes only, $CHCl_3$ exhibits the second highest flux
558 of all investigated VHOCs (175 nmol m^{-2} s^{-1}), suggesting both high emission and their balance
559 to some extent by sinks for this species.

560 Natural emission of trihalomethanes from soil has been shown to occur without microbial
561 activity involvement, induced via oxidation of organic matter by an electron acceptor such as
562 Fe(III) (Huber et al., 2009) or via hydrolysis of trihaloacetyl compounds (Albers et al., 2017).
563 The soils studied by Albers et al. (2017) are in general significantly richer in OM than the soil at
564 the Dead Sea, except for COAST−TKM-SD. Hence, the apparently higher emission from the
565 Dead Sea soil may indicate either a different mechanism leading to the release of
566 trihalomethanes from soil or only a weak dependency on availability of OM in the soil. The
567 latter possibility may be supported by the fact that Albers et al. (2017) did not find a correlation
568 between chloroform emission rate and organic chlorine in the soil, and by the association found
569 in the present study between soil halide content and VHOC flux for COAST−EGD and
570 COAST−TKM sites (Sect 3.2.2). While trihalomethane formation via organic matter oxidation
571 was reported to occur more rapidly at low pH, and specifically at pH > ~3.5 (Huber et al.,
572 2009;Ruecker et al., 2014), its formation via hydrolysis of trihaloacetyl is expected to occur
573 faster at the relatively high pH of ≥ 7 (Hoekstra et al., 1998;Albers et al., 2017). Yet, according
574 to Ruecker et al. (2014), in hypersaline sediments the formation of VHOCs via organic matter
575 oxidation involving Fe(III) can occur at pH > 8 for biotic processes. Therefore, given the
576 relatively high pH (~7.4−7.9) at these sites, our present findings of high trihalomethane

577 emission rates from bare and from vegetated soil sites support the evidence supplied by Albers
578 et al. (2017) concerning the emission of trihalomethanes from the soil after trihaloacetyl
579 hydrolysis (Table 3). Albers et al. (2017) demonstrated that their proposed mechanism supports
580 the emission of $CHCl_3$ and $CHBrCl_2$ from soil, and suggested that additional halomethanes with
581 higher number of bromine atoms can be expected to be emitted via this mechanism, but at much
582 lower rates. Hence, the higher net fluxes for $CHBr_2Cl$ and $CHBr_3$ at the Dead Sea could occur
583 either because of the markedly higher composition of different halides in the Dead Sea soil (see
584 Table 3) or because another mechanism is also playing a role in the emission. The finding of
585 Hoekstra et al. (1998) that bromine enrichment mainly enhances the emission of $CHBr_3$ and
586 $CHBr_2Cl$ rather than that of $CHBrCl_2$ supports the former possibility. While both Cl and Br soil
587 contents are relatively high for the SD and COAST-EGD-MD, where emission of brominated
588 trihalomethanes was higher than that of chlorinated trihalomethanes (see Table 4), remarkably
589 high Br/Cl (1:43) relative to other sites was found in COAST−TKM-SD. No clearly more
590 elevated positive flux of brominated compared to chlorinated trihalomethanes was observed for
591 this site, suggesting that the main reason for the relatively elevated brominated trihaloethanes at
592 the SD sites and COAST−EGD-MD is the high Br content rather than the Br/Cl ratio. The
593 relatively elevated net flux of brominated trihalomethanes from the soil and vegetated sites
594 indicates that relatively high rates of emission of these species can also occur from soils that are
595 much less rich in Br than the SD sites and COAST−EGD-MD sites (see Tables 3, 4). Yet, the
596 emission rates of $CHBrCl_2$ at the Dead Sea were generally higher than those observed by Albers
597 et al. (2017), probably reflecting the higher chlorine soil content at the Dead Sea.

598 Methyl halides: Similarly to $CHCl_3$, the methyl halides CH_3Cl, CH_3Br, and CH_3I exhibit
599 relatively large differences between their average overall measured fluxes and the average
600 positive flux, implying high rates of both emission and deposition. The average positive flux of
601 CH_3Cl is the highest of all the VHOCs investigated, indicating strong emission and deposition
602 for this species at the Dead Sea. Several studies have indicated that soil tends to act as a sink for

603 CH_3Cl (Rhew et al., 2003). The relatively high fluxes of CH_3Cl and CH_3Br at WM−KLY-1 (983
604 and 53.5 nmol m^{-2} d^{-1}, respectively) may point to emission of this species from the local
605 vegetation, in agreement with previous studies (Sect. 1), and potentially caused by a microbial-
606 or fungal-induced emission (Moore et al., 2005;Watling and Harper, 1998).

607 A positive net flux for CH_3I was observed at least once at each of the vegetated soils, bare
608 soils, or soils mixed with salt deposit mixtures (Table 4), but the fluxes we observed were not
609 significantly higher than those obtained in previous studies (Sect. 3.1), a finding that might be
610 attributable to the small concentrations of I in the soil relative to those of the other halides. At
611 Duke Forest, Sive et al. (2007) observed a soil-emission CH_3I flux of ~0.27 nmol m^{-2} d^{-1} on
612 average (ranging from ~ 0.11 to 0.31 nmol m^{-2} d^{-1}) under precipitation conditions in June, and
613 higher emission rates (0.8 and 4.1 nmol m^{-2} d^{-1}) under warmer and dryer conditions in
614 September. In agreement with those findings, although generally our analyses did not indicate
615 clear seasonal effects, we found that in all cases the net CH_3I fluxes were higher in spring than
616 in winter, except for COAST−TKM-SD (Fig. 2). Also, in 83 % of the measurements the CH_3I
617 mixing ratios were higher in spring than in winter (Fig. 3).

618 Relatively high fluxes of CH_3Cl and CH_3Br, and to a lesser extent of CH_3I, were observed at
619 the COAST−TKM and COAST−EGD sites, particularly from the sites closest to the seawater.
620 According to Keppler et al. (2000), the presence of Fe(III), OM and halide ions are basically
621 sufficient to result in emission of methyl halides from both soil and sediments by a natural
622 abiotic process (Sect.1). The strong emission of methyl halide from the COAST−TKM and
623 COAST−EGD sites indicates that these species can be emitted at high rates from saline soil that
624 is not rich in OM. The strongest emissions occurred from COAST−TKM-SD, COAST−EGD-
625 SD and to some extent from COAST−EGD-MD, pointing to a high sensitivity of methyl halide
626 emission to soil OM and/or halide content (see Table 3). However, the emission of methyl
627 halides from COAST−TKM-SD, where soil OM is substantially higher than at all other

investigated sites, is similar to or lower than the emission from COAST−EGD-SD and COAST−EGD-MD.

In a study of emissions of the three methyl halides from soil by controlled experiments, Keppler et al. (2000) found a decrease in the efficiency of methyl halide emission according to $CH_3I > CH_3Br > CH_3Cl$ (10:1.5:1; mole fractions). We estimated the emission efficiencies of the different methyl halides based on the ratio between their fluxes and the concentrations of halide in the soil. To maintain consistency with the calculations of Keppler et al. (2000) our calculation was also based on mole fractions, and took into account only positive fluxes, on the assumption that they are closer in magnitude to emission. This corresponded with measured soil halide concentration proportions for Cl:B:I as 38487:445:1, and the evaluated emission efficiency proportions were 57.7:1.56:1 for CH_3I, CH_3Br and CH_3Cl, respectively. These calculations verify an increasing efficiency of methyl halide emission such that $CH_3Cl < CH_3Br < CH_3I$, in agreement with Keppler et al. (2000). These findings suggest that the methylation and emission of CH_3Br and CH_3Cl in our study were controlled by abiotic mechanisms similar to those reported by Keppler et al. (2000). The apparently higher relative efficiency of CH_3I emission may point to emissions of CH_3I via other mechanisms in the studied area, as discussed in Sect. 3.3. It should be noted, however, that we based our calculations on positive flux and not emission flux, which might also be a reason for the inconsistency between relative emission efficiency of CH_3I calculated by Keppler et al. (2000) and by us.

C_2HCl_3: Only COAST−EGD was found to be, on average, a source for C_2HCl_3, mostly derived from strong emissions from COAST−EGD-SD (see, e.g., Fig. 2). COAST−EGD-SD is a mixture of salt beds with salty soil and therefore the elevated emissions of C_2HCl_3 at this site appear to support previous evidence for the emission of this gas by halobacteria from salt lakes, as reported by Weissflog et al. (2005). Additional chlorinated VHOCs, including $CHCl_3$ and CH_3Cl, also demonstrated increased emission from this site, in line with the findings of Weissflog et al. (2005). Note that the net measured fluxes for most of the VHOCs investigated

654 during COAST−EGD-SD-w were smaller than those of COAST−EGD-SD-s, as discussed in
655 Sect. 3.2.2.

656 CH_2Br_2: CH_2Br_2 showed positive fluxes from all site types, with a positive average net flux
657 from most sites (see Fig. 2). The highest fluxes were observed over TMRX−ET (TMRX−ET-2)
658 and over bare soil (BARE−MSD-2). Correlation of CH_2Br_2 with trihalomethanes will be
659 discussed in Sect. 3.3

660

661 **3.3 Flux and mixing ratio correlations between VHOCs**

662 Table 5 presents the correlations between the evaluated mixing ratios of VHOCs at the Dead
663 Sea**,** separately for all sites and for the terrestrial sites only. In most cases the correlations
664 between species over the terrestrial sites were low ($r^2 < 0.1$), but were substantially higher for
665 the brominated trihalomethanes ($CHBr_3$−$CHBrCl_2$ ($r^2 = 0.62$), $CHBr_2Cl$−$CHBrCl_2$ ($r^2 = 0.75$),
666 and $CHBr_2Cl$−$CHBr_3$ ($r^2 = 0.72$), supporting a common source mechanism for these species.
667 Relatively high correlations were also obtained, although to a lesser extent, between methyl
668 halides, particularly between CH_3Cl and CH_3Br ($r^2 = 0.57$). Correlations were in most cases
669 either similar or smaller, when we included measurements over the seawater site SEA−KDM,
670 which may reinforce predominant contribution of VHOCs from terrestrial sources in the area of
671 the Dead Sea. Table 5 shows relatively high correlations of $CHCl_3$ with all the methyl halides
672 CH_3Cl, CH_3Br and CH_3I (with r^2 ranging from 0.19 to 0.28), suggesting common emission
673 sources and/or sinks for these species.

Atmos. Chem. Phys. Discuss., https://doi.org/10.5194/acp-2018-1172
Manuscript under review for journal Atmos. Chem. Phys.
Discussion started: 17 December 2018

Atmospheric Chemistry and Physics Discussions

674 **Table 5.** Correlations between the mixing ratios of VHOCs. Shown is the coefficient of determination (r^2) between
675 each VHOC pair for the measured mixing ratio, when calculated over all sites excluding SEA−KDM and including
676 SEA−KDM (in parenthesis).

	$CHBrCl_2$	**$CHBr_3$**	**$CHBr_2Cl$**	**$CHCl_3$**	**CH_2Br_2**	**C_2HCl_3**	**CH_3Cl**	**CH_3Br**
CH_3I	0.05 (0.05)	0.02 (0.02)	0.02 (0.02)	0.20 (0.21)	0.01 (0.01)	0.03 (0.03)	0.09 (0.10)	0.13 (0.13)
CH_3Br	0.04 (0.03)	0.14 (0.14)	0.07 (0.06)	0.19 (0.18)	0.27 (0.26)	0.04 (0.03)	0.57 (0.56)	
CH_3Cl*	0.00 (0.00)	0.05 (0.04)	0.02 (0.02)	0.28 (0.28)	0.01 (0.01)	0.01 (0.01)		
C_2HCl_3	0.01 (0.01)	0.03 (0.01)	0.02 (0.03)	0.07 (0.07)	0.00 (0.00)			
CH_2Br_2	0.00 (0.00)	0.05 (0.04)	0.01 (0.01)	0.03 (0.03)				
$CHCl_3$	0.13 (0.13)	0.07 (0.04)	0.06 (0.06)					
$CHBr_2Cl$	0.75 (0.76)	0.72 (0.56)						
$CHBr_3$	0.62 (0.48)							

677 *Correlations for CH_3Cl over VEG sites were excluded one CH_3Cl measurement in TMRX−ET-1 (see Sect. 2.1.2).

678 Table 6 records the correlations between the measured VHOC fluxes, separately for all sites,
679 bare soil sites, vegetated sites (VEG), TMRX−ET sites and WM−KLY sites, as well as for the
680 sites closer to the seawater, including all COAST−TKM and COAST−EGD sites. For the two
681 last, correlations are also presented separately for the two SD sites closest to the seawater
682 (COAST−TKM-SD and COAST−EGD-SD). Note that the table compares net flux rather than
683 emission flux, and therefore the reported correlations are expected to be affected by both sinks
684 and sources for the different VHOCs.

685 Table 6 demonstrates moderate to high positive correlations in most cases when all sites are
686 included in the calculation, while in general the correlations were significantly higher when
687 calculated for sites of the same type, suggesting common emission mechanisms or controls. In
688 most cases correlations for the vegetated sites were higher than the overall correlations for all
689 sites. The relatively high correlations in the vegetated sites may be in line with previous studies
690 indicating high emissions from vegetation at marsh coasts (Rhew et al., 2002;Deventer et al.,
691 2018), but positive fluxes for methyl halides were obtained only in a few cases at the vegetated
692 sites, and not in all cases for all methyl halides simultaneously. Hence, it appears that the

693 correlations between methyl halides at the vegetated sites are more likely to be attributable to
694 common sinks. The fairly elevated correlations between methyl halide fluxes at the SD sites,
695 together with the fact that, in most cases, fluxes of the three methyl halides from these sites were
696 positive and high, suggests that these sites have a common source or sources for methyl halides.

697 High correlations were obtained for trihalomethanes in the vegetated sites ($r \geq 0.82$), except
698 for $CHCl_3$, whose correlations with other trihalomethanes were lower. We also observed high
699 correlations of CH_2Br_2 with all trihalomethanes, particularly for the vegetated sites ($r \geq 0.77$),
700 and somewhat lower correlations with $CHCl_3$ ($r = 0.55$). CH_2Br_2 also showed high correlations
701 with $CHBrCl_2$ ($r = 0.90$) and $CHBr_3$ ($r = 0.88$) at the SD sites, suggesting a common emission
702 mechanism for CH_2Br_2 and the other trihalomethanes.

703 Correlation of CH_2Br_2 with $CHBr_2Cl$ at the SD sites was strongly negative ($r = -0.93$),
704 similarly to the negative correlation between $CHBr_2Cl$ and the other brominated
705 trihalomethanes, $CHBCl_2$ ($r = -0.98$) and $CHBr_3$ ($r = -0.65$), at these sites. This, together with
706 the fact that the measured fluxes of these species were generally positive over the SD sites,
707 points to competitive emission between $CHBr_2Cl$ and both $CHBrCl_2$ and $CHBr_3$, at least at the
708 SD sites. This is supported by the analysis in Sects. 3.2.2 and 3.2.3, which have demonstrated
709 that the halide content of the soil appears to play a major role in controlling the emission rates of
710 VHOCs under the studied conditions. High positive correlation between all four brominated
711 species was observed for the bare soil sites as well as for the vegetated sites (see Table 6),
712 further supporting the notion that $CHBr_2Cl$ too can be emitted via mechanisms similar to those
713 of the other two brominated trihalomethanes and CH_2Br_2.

714 Table 6 also indicates overall low correlations between $CHCl_3$ and all of the brominated
715 trihalomethanes, mostly resulting from negative correlations at the bare soil sites. There was
716 also a higher incidence of positive fluxes at the bare soil sites for the trihalomethanes $CHCl_3$ and
717 $CHBrCl_2$, compared with the less chlorinated, $CHBr_3$ and $CHBr_2Cl$ (Table 4). Hence, the
718 negative correlation between $CHCl_3$ and the brominated trihalomethanes at the bare soil sites

719 may indicate competitive emission between the more chlorinated and the more brominated
720 trihalomethanes. The situation at the bare soil sites resembles previous reports of the
721 predominant emission of $CHCl_3$ at the expense of the more brominated species (e.g., (Albers et
722 al., 2017;Huber et al., 2009)), particularly $CHBr_3$ and $CHBr_2Cl$. This would be expected, given
723 the higher Cl/Br ratio at these sites (see Table 3). We should emphasize that even at the bare soil
724 sites we observed relatively high positive fluxes of brominated trihalomethanes, which would
725 not generally be expected (Albers et al., 2017), and can be attributed to the relatively high
726 bromine enrichment of the soil.

727 Interestingly, in agreement with Table 5, Table 6 also shows relatively high correlations
728 between $CHCl_3$ and all methyl halides, particularly for BARE ($r \geq 0.68$) and at the SD sites ($r \geq$
729 0.59). We also found high correlations for the SD sites between C_2HCl_3 and all methyl halides (r
730 $\geq$ 0.59). Remarkably high correlations were obtained between CH_3I and the brominated
731 trihalomethanes and CH_2Br_2 at the vegetated sites ($r \geq 0.57$), and for CH_3I with $CHCl_3$ and
732 C_2HCl_3 at the SD sites ($r = 0.99$ in both cases). In most cases the flux of CH_3I was negative at
733 the vegetated sites; therefore, it is not clear whether the strong correlations between CH_3I and
734 the brominated trihalomethanes at these sites point to common sources or sinks. In contrast,
735 positive fluxes of both CH_3I and the brominated trhihalomethanes and CH_2Br_2 were observed at
736 the SD sites in most cases, pointing to a common source of these species at the SD sites.
737 Weissflog et al. (2005) found that emission of C_2HCl_3, $CHCl_3$ and other chlorinated VHOCs can
738 occur from salt lakes via the activity of halobacteria in the presence of dissolved Fe (III) and
739 crystallized NaCl. The strong correlations of $CHCl_3$, C_2HCl_3 and CH_3I ($r = 0.99$ in all cases)
740 reinforce the common emission of $CHCl_3$ and C_2HCl_3 from salt lake sediments, as indicated by
741 Weissflog et al. (2005), and may also indicate that CH_3I can be emitted in a similar way. The
742 fact that the emission of CH_3I in our study was much more efficient than under the conditions
743 used by Keppler et al. (2000) supports the possibility that mechanisms other than the abiotic
744 emission pathway proposed by Keppler et al. (2000) influence the emission of CH_3I at the Dead

Atmos. Chem. Phys. Discuss., https://doi.org/10.5194/acp-2018-1172
Manuscript under review for journal Atmos. Chem. Phys.
Discussion started: 17 December 2018

Atmospheric Chemistry and Physics Discussions

745 Sea (Sect. 3.2.3). The relatively high correlations between fluxes of $CHCl_3$ and C_2HCl_3 and the
746 other methyl halides, CH_3Br and CH_3Cl, for Bare and SD, may suggest that these methyl halides
747 are also emitted, via similar mechanisms, from the salt deposits.

748

749 **Table 6.** Correlations between the measured net flux of VHOCs. The table records the Pearson correlation
750 coefficient (r) for the measured net flux between each VHOC pair, calculated over all sites except SEA−KDM.

		$CHBrCl_2$	$CHBr_3$	$CHBr_2Cl$	$CHCl_3$	CH_2Br_2	C_2HCl_3	CH_3Cl	CH_3Br
CH_3I	All (n = 20)	**0.34**	**0.13**	**-0.56**	**0.58**	**0.19**	**0.59**	**0.45**	**0.23**
	BARE (n = 6)	-0.54	-0.85	-0.78	0.68	-0.32	0.54	0.73	0.77
	COAST (n = 10)	0.50	0.26	-0.64	0.66	0.81	0.63	0.54	0.08
	SD (n = 4)	(0.13)	(0.72)	(-0.05)	(0.99)	(0.35)	(0.99)	(0.90)	(0.69)
	VEG (n = 4)	0.76	0.72	0.57	0.31	0.88	0.16	0.11	0.45
CH_3Br	All (n = 20)	**-0.08**	**0.39**	**0.22**	**0.20**	**-0.06**	**0.33**	**0.30**	
	BARE (n = 6)	-0.22	-0.83	-0.45	0.83	-0.21	0.57	0.61	
	COAST (n = 10)	-0.51	0.65	0.19	0.29	-0.04	0.33	-0.24	
	SD (n = 4)	(-0.62)	(0.07)	(0.69)	(0.59)	(-0.40)	(0.59)	(0.69)	
	VEG (n = 4)	0.67	0.87	0.47	-0.57	0.36	-0.76	0.94	
CH_3Cl*	All (n = 19)	**0.27**	**0.05**	**0.00**	**-0.37**	**-0.15**	**0.54**		
	BARE (n = 6)	-0.33	-0.63	-0.54	0.86	0.21	0.71		
	COAST (n = 10)	0.58	-0.09	-0.16	0.69	0.14	0.66		
	SD (n = 4)	(0.07)	(0.45)	(0.08)	(0.91)	(0.12)	(0.86)		
	VEG (n = 3)	0.45	0.68	0.31	-0.75	0.06	-0.91		
C_2HCl_3	All (n = 20)	**0.10**	**0.53**	**0.05**	**0.83**	**0.02**			
	Bare (n = 6)	-0.41	-0.66	-0.52	0.56	-0.10			
	COAST (n = 10)	0.30	0.65	-0.01	0.99	0.26			
	SD (n = 4)	(0.26)	(0.81)	(-0.19)	(0.99)	(0.48)			
	VEG (n = 4)	-0.05	-0.34	0.12	0.96	0.33			
CH_2Br_2	All (n = 20)	**0.62**	**0.36**	**-0.17**	**0.15**				
	BARE (n = 6)	0.77	0.58	0.68	0.08				
	COAST (n = 10)	0.45	0.26	-0.85	0.27				
	SD (n = 4)	(0.90)	(0.88)	(-0.93)	(0.45)				
	VEG (n = 4)	0.91	0.77	0.87	0.55				
$CHCl_3$	All (n = 20)	**0.01**	**0.30**	**0.01**					
	BARE (n = 6)	-0.25	-0.74	-0.46					
	COAST (n = 10)	0.31	0.60	-0.04					
	SD (n = 4)	(0.27)	(0.77)	(-0.18)					
	VEG (n = 4)	0.22	-0.09	0.40					
$CHBr_2Cl$	All (n = 20)	**-0.11**	**0.16**						
	Bare (n = 6)	0.95	0.86						
	COAST (n = 10)	-0.22	0.11						
	SD (n = 4)	(-0.98)	(-0.65)						
	VEG (n = 4)	0.82	0.94						
$CHBr_3$	All (n = 20)	**0.22**							
	BARE (n = 6)	0.72							
	COAST (n = 10)	-0.04							
	SD (n = 4)	(0.65)							
	VEG (n = 4)	0.95							

751 * Correlations for CH_3Cl over VEG sites were excluded one CH_3Cl measurement in TMRX−ET-1 (see Sect.
752 2.1.2).

Atmos. Chem. Phys. Discuss., https://doi.org/10.5194/acp-2018-1172
Manuscript under review for journal Atmos. Chem. Phys.
Discussion started: 17 December 2018

Atmospheric Chemistry and Physics Discussions

Summary

The results of this study demonstrate high emission rates of the investigated methyl halides as well as of brominated and chlorinated VSLS at the Dead Sea area, corresponding with mixing ratios which in most cases are significantly higher than typical values in the MBL. Overall, our measurements indicate a higher incidence (in 65−85 % of measurements) of positive fluxes of brominated than of chlorinated VHOCs, except for $CHCl_3$, for which the incidence of positive net fluxes was also relatively high (65 % of measurements). The high incidence of brominated VHOCs can be attributed primarily to the relatively large amount of Br in the soil, rather than the Br/Cl ratio. We did not detect any clear effect of meteorological parameters, emission from the seawater, or season, other than — in agreement with Sive et al. (2007) — an apparently higher emission of CH_3I during spring than during winter. The four investigated site types, the cultivated and natural vegetated, the bare soil and the coastal sites, are identified as potential net sources for all VHOCs investigated, except for the emission of CH_3I and C_2HCl_3 from the vegetated sites. Hence, this study reveals strong emission of VHOCs over at least a few kilometers from the Dead Sea. The fluxes, in general, were highly variable, showing changes between sampling periods even for a specific species at a specific site.

Emissions were highest from the SD sites, where salinity is maximal, and which clearly showed an increased incidence of positive flux with decreasing distance from the seawater, pointing to the sensitivity of VHOC emission rates to salinity even at the hypersaline coastal area of the Dead Sea. The measurements did not indicate either increased or reduced emissions of VHOCs from the seawater itself. It was shown that emissions of VHOCs can occur from dry soil under semi-arid conditions during summer, in agreement with findings from other geographic locations that soil water does not seem to be a limiting factor in VHOC emission (Kotte et al., 2012). Rain events appear to attenuate the emission rates of VHOCs at the Dead Sea. Measurements at a bare soil site suggested a decrease in VHOC emission rates for 1−3 days

778 after a rain event, while the gradual increase in VHOC emission more than three days after the
779 rain event suggests that these VHOC emissions are, at least partially, biotic-induced.

780 Trihalomethanes, including $CHCl_3$, $CHBr_2Cl$, $CHBr_3$ and particularly $CHBrCl_2$, are
781 associated with the highest number of sites at which their flux was, on average, positive, while
782 $CHBr_3$, $CHBr_2Cl$ and $CHBrCl_2$ showed relatively high incidence of positive fluxes, with values
783 of 65 %, 80 % and 85 %, respectively. This finding, together with the relatively high
784 correlations observed between brominated trihalomethanes, points to common formation and
785 emission mechanisms of these brominated trihalomethanes, in line with previous studies. Our
786 analyses further suggest emission of CH_2Br_2 via mechanisms that are common to the
787 trihalomethanes. Correlation of the brominated trihalomethanes with $CHCl_3$ was lower. Whereas
788 Albers et al. (2017) suggested that $CHBr_3$ and $CHBr_2Cl$ are emitted from soil only in relatively
789 small amounts compared to $CHCl_3$, our results point to their higher emission via common
790 mechanisms with the other trihalomethanes. The overall average net flux of the trihalomethanes
791 decreased according to $CHBr_2Cl$ > $CHBr_3$ > $CHBrCl_2$ > $CHCl_3$. The enhanced emission of
792 brominated trihalomethanes probably reflects the enrichment of the Dead Sea soil with bromine,
793 in line with findings by Hoekstra et al. (1998), who identified a higher natural emission of
794 $CHBr_3$ and $CHBr_2Cl$ rather than of $CHBrCl_2$ from the soil, following the soil's enrichment with
795 KBr.

796 We identified the SD sites as a probable source for all methyl halides, whereas vegetated
797 sites appear more likely to act as a net sink for these species. Comparing the proportion of Br
798 and Cl in the soil for the various sites with proportions of measured positive flux of CH_3Br and
799 CH_3Cl are in line with reports by Keppler et al. (2001) about emission of methyl halides via
800 abiotic oxidation of organic matter in the soil. Similar calculations in our study demonstrated
801 much higher efficiencies of CH_3I emission than those reported by Keppler et al. (2000), pointing
802 to emission of CH_3I via other mechanisms. The high correlation of CH_3I emission with that of
803 $CHCl_3$ and C_2HCl_3, particularly at the SD sites, together with findings by Weissflog et al.

(2005), of various chlorinated VHOCs emission, including $CHCl_3$ and C_2HCl_3, from salt lake sediments, suggests that the Dead Sea, particularly the SD, sites probably act as an emission source for $CHCl_3$, C_2HCl_3 and CH_3I via similar mechanisms. Weissflog et al. (2005) reported that the emission of chlorinated VHOCs in their study was induced by microbial activity. Keppler et al. (2000) reported the involvement of an abiotic process in the formation of alkyl from soil and sediments, and the observed correlation between methyl halides and both $CHCl_3$ and C_2HCl_3 may indicate that the two processes occur simultaneously. Further research will be needed to decipher the relative importance of each process in soil and salt sediments, including more direct emission measurements from a better-defined landform, e.g., by using flux chambers.

Of all the VHOCs investigated in our study, $CHBr_3$ showed the highest enrichment with respect to MBL mixing ratios. Owing to the relatively short tropospheric lifetime of $CHBr_3$, its photolysis contributes significantly to reactive bromine formation in the MBL. However, although relatively high, the elevated $CHBr_3$ fluxes and mixing ratios that we measured at the Dead Sea, cannot lead to the elevated mixing ratios of reactive bromine species at the Dead Sea, which are frequently associated with BrO > 100 ppt (e.g., see Matveev et al. (2001) and Tas et al. (2005)). Similarly, if CH_3I photolysis is the only source of reactive iodine species, the measured fluxes and elevated mixing ratios of CH_3I are not high enough to account for the high IO in this area. Given their relatively fast photolysis, however, CH_3I and $CHBr_3$, as well as CH_2Br_2, may well have roles to play in the initiation of reactive bromine and iodine formation in this area.

Overall, along with other studies, the findings presented here highlight the potentially important role played by emission of VHOCs from saline soil and salt lakes in stratospheric and tropospheric chemistry, and call for further research on VHOC emission rates and controlling mechanisms.

Data availability. Data are available upon request from the corresponding author Eran Tas (eran.tas@mail.huji.ac.il).

Author *contribution:* ET, AG and RR designed the experiments. MS, GL and QL carried the field measurements out and DB carried out the sampled air analysis. GL contributed in designing and constructing a special mechanism for simultaneous lifting and dropping of sampling canisters. Data curation and formal analysis were performed by ET and MS with support from RR. ET and MS and ET prepared the manuscript with contributions from all co-authors.

Competing interests. The authors declare that they have no conflict of interest**.**

Acknowledgements

This study was supported by United States−Israel Binational Science Foundation (Grant 2012287). E.T. holds the Joseph H. and Belle R. Braun Senior Lectureship in Agriculture.

References

Albers, C. N., Jacobsen, O. S., Flores, E. M. M., and Johnsen, A. R.: Arctic and Subarctic Natural Soils Emit Chloroform and Brominated Analogues by Alkaline Hydrolysis of Trihaloacetyl Compounds, Environ Sci Technol, 51, 6131-6138, 10.1021/acs.est.7b00144, 2017.

Alpert, P., Shafir, H., and Issahary, D.: Recent changes in the climate at the dead sea - A preliminary study, Climatic Change, 37, 513-537, Doi 10.1023/A:1005330908974, 1997.

Bondu, S., Cocquempot, B., Deslandes, E., and Morin, P.: Effects of salt and light stress on the release of volatile halogenated organic compounds by Solieria chordalis: a laboratory incubation study, Botanica Marina, 51, 485-492, 10.1515/Bot.2008.056, 2008.

Breider, F., and Albers, C. N.: Formation mechanisms of trichloromethyl-containing compounds in the terrestrial environment: A critical review, Chemosphere, 119, 145-154, 10.1016/j.chemosphere.2014.05.080, 2015.

Brinckmann, S., Engel, A., Bonisch, H., Quack, B., and Atlas, E.: Short-lived brominated hydrocarbons - observations in the source regions and the tropical tropopause layer, Atmos Chem Phys, 12, 1213-1228, 10.5194/acp-12-1213-2012, 2012.

Buchalo, A. S., Nevo, E., Wasser, S. P., Oren, A., and Molitoris, H. P.: Fungal life in the extremely hypersaline water of the Dead Sea: first records, P Roy Soc B-Biol Sci, 265, 1461-1465, DOI 10.1098/rspb.1998.0458, 1998.

Butler, J. H., King, D. B., Lobert, J. M., Montzka, S. A., Yvon-Lewis, S. A., Hall, B. D., Warwick, N. J., Mondeel, D. J., Aydin, M., and Elkins, J. W.: Oceanic distributions and emissions of short-lived halocarbons, Global Biogeochem Cy, 21, Artn Gb102310.1029/2006gb002732, 2007.

Carpenter and Reimann, L. A., J.B. Burkholder, C. Clerbaux, B.D. Hall, R., et al., and Hossaini, J. C. L., and S.A. Yvon-Lewis: Ozone-depleting substances (ODSs) and other gases of interest to the Montreal Protocol, Chapter 1 in Scientific Assessment of Ozone Depletion: 2014, Global Ozone Research and Monitoring Project – Report No. 55, World Meteorological Organization, Geneva, Switzerland, 2014.

Carpenter, L. J., Green, T. J., Mills, G. P., Bauguitte, S., Penkett, S. A., Zanis, P., Schuepbach, E., Schmidbauer, N., Monks, P. S., and Zellweger, C.: Oxidized nitrogen and ozone production efficiencies in the springtime free troposphere over the Alps, J Geophys Res-Atmos, 105, 14547-14559, Doi 10.1029/2000jd900002, 2000.

Carpenter, L. J., Wevill, D. J., O'Doherty, S., Spain, G., and Simmonds, P. G.: Atmospheric bromoform at Mace Head, Ireland: seasonality and evidence for a peatland source, Atmos Chem Phys, 5, 2927-2934, DOI 10.5194/acp-5-2927-2005, 2005.

Carpenter, L. J., Jones, C. E., Dunk, R. M., Hornsby, K. E., and Woeltjen, J.: Air-sea fluxes of biogenic bromine from the tropical and North Atlantic Ocean, Atmos Chem Phys, 9, 1805-1816, 2009.

Carpenter, L. J., MacDonald, S. M., Shaw, M. D., Kumar, R., Saunders, R. W., Parthipan, R., Wilson, J., and Plane, J. M. C.: Atmospheric iodine levels influenced by sea surface emissions of inorganic iodine, Nature Geoscience, 6, 108-111, 10.1038/Ngeo1687, 2013.

Colman, J. J., Swanson, A. L., Meinardi, S., Sive, B. C., Blake, D. R., and Rowland, F. S.: Description of the analysis of a wide range of volatile organic compounds in whole air samples collected during PEM-Tropics A and B, Analytical Chemistry, 73, 3723-3731, DOI 10.1021/ac010027g, 2001.

Dearellano, J. V. G., Duynkerke, P. G., and Zeller, K. F.: Atmospheric Surface-Layer Similarity Theory Applied to Chemically Reactive Species, J Geophys Res-Atmos, 100, 1397-1408, Doi 10.1029/94jd02434, 1995.

Derendorp, L., Wishkerman, A., Keppler, F., McRoberts, C., Holzinger, R., and Rockmann, T.: Methyl chloride emissions from halophyte leaf litter: Dependence on temperature and chloride content, Chemosphere, 87, 483-489, 10.1016/j.chemosphere.2011.12.035, 2012.

Deventer, M. J., Jiao, Y., Knox , S. H., Anderson , F., Ferner, M. C., Lewis, J. A., and Rhew, R. C.: Ecosystem-Scale Measurements of Methyl Halide Fluxes From a Brackish Tidal Marsh Invaded With Perennial Pepperweed (Lepidium latifolium), J Geophys Res-Atmos-Biogeosciences, 10.1029/2018JG004536, 2018.

Dimmer, C. H., Simmonds, P. G., Nickless, G., and Bassford, M. R.: Biogenic fluxes of halomethanes from Irish peatland ecosystems, Atmos Environ, 35, 321-330, Doi 10.1016/S1352-2310(00)00151-5, 2001.

Dyer, A. J., and Bradley, E. F.: An Alternative Analysis of Flux-Gradient Relationships at the 1976 Itce, Bound-Lay Meteorol, 22, 3-19, Doi 10.1007/Bf00128053, 1982.

Ekdahl, A., Pedersen, M., and Abrahamsson, K.: A study of the diurnal variation of biogenic volatile halocarbons, Mar Chem, 63, 1-8, Doi 10.1016/S0304-4203(98)00047-4, 1998.

Gan, J., Yates, S. R., Ohr, H. D., and Sims, J. J.: Production of methyl bromide by terrestrial higher plants, Geophys Res Lett, 25, 3595-3598, Doi 10.1029/98gl52697, 1998.

Gebhardt, S., Colomb, A., Hofmann, R., Williams, J., and Lelieveld, J.: Halogenated organic species over the tropical South American rainforest, Atmos Chem Phys, 8, 3185-3197, 2008.

Gifford, F. A.: Turbulent diffusion typing schemes: A review," under (R. L. Schoup, Ed.) "Consequences of Effluent Release, Nucl. Safety 17 (l), 6846,1976.

EPA, United States Environmental Protection Agency Meteorological Monitoring Guidance for Regulatory Modeling Applications, 2000.

Golder D.: Relations among stability parameters in the surface layer ;3(1):47–58., Boundary-Layer Meteorol, 31, 47-58, 1972.

Gualtieri, G., and Secci, S.: Comparing methods to calculate atmospheric stability-dependent wind speed profiles: A case study on coastal location, Renew Energ, 36, 2189-2204, 10.1016/j.renene.2011.01.023, 2011.

916 Hebestreit, K., Stutz, J., Rosen, D., Matveiv, V., Peleg, M., Luria, M., and Platt, U.: DOAS measurements
917 of tropospheric bromine oxide in mid-latitudes, Science, 283, 55-57, DOI
918 10.1126/science.283.5398.55, 1999.
919 Hoekstra, E. J., De Leer, E. W. B., and Brinkman, U. A. T.: Natural formation of chloroform and
920 brominated trihalomethanes in soil, Environ Sci Technol, 32, 3724-3729, DOI
921 10.1021/es980127c, 1998.
922 Hossaini, R., Chipperfield, M. P., Monge-Sanz, B. M., Richards, N. A. D., Atlas, E., and Blake, D. R.:
923 Bromoform and dibromomethane in the tropics: a 3-D model study of chemistry and
924 transport, Atmos Chem Phys, 10, 719-735, 10.5194/acp-10-719-2010, 2010.
925 Hossaini, R., Mantle, H., Chipperfield, M. P., Montzka, S. A., Hamer, P., Ziska, E., Quack, B., Kruger, K.,
926 Tegtmeier, S., Atlas, E., Sala, S., Engel, A., Bonisch, H., Keber, T., Oram, D., Mills, G., Ordonez,
927 C., Saiz-Lopez, A., Warwick, N., Liang, Q., Feng, W., Moore, E., Miller, B. R., Marecal, V.,
928 Richards, N. A. D., Dorf, M., and Pfeilsticker, K.: Evaluating global emission inventories of
929 biogenic bromocarbons, Atmos Chem Phys, 13, 11819-11838, 10.5194/acp-13-11819-2013,
930 2013.
931 Huber, S. G., Kotte, K., Scholer, H. F., and Williams, J.: Natural Abiotic Formation of Trihalomethanes in
932 Soil: Results from Laboratory Studies and Field Samples, Environ Sci Technol, 43, 4934-4939,
933 10.1021/es8032605, 2009.
934 IPCC (Ed.) Contribution of Working Group I to the Fourth Assessment Report of the Intergovernmental
935 Panel on Climate Change. , Cambridge University Press, Cambridge, United Kingdom and New
936 York, NY, USA, 2007.
937 Jacob, J. H., Hussein, E. I., Shakhatreh, M. A. K., and Cornelison, C. T.: Microbial community analysis of
938 the hypersaline water of the Dead Sea using high-throughput amplicon sequencing,
939 Microbiologyopen, 6, ARTN e50010.1002/mbo3.500, 2017.
940 Keppler, F., Eiden, R., Niedan, V., Pracht, J., and Scholer, H. F.: Halocarbons produced by natural
941 oxidation processes during degradation of organic matter, Nature, 403, 298-301, Doi
942 10.1038/35002055, 2000.
943 Keppler, F., Eiden, R., Niedan, V., Pracht, J., and Scholer, H. F.: Halocarbons produced by natural
944 oxidation processes during degradation of organic matter (vol 403, pg 298, 2000), Nature, 409,
945 382-+, DOI 10.1038/35053144z, 2001.
946 Khan, M. A. H., Whelan, M. E., and Rhew, R. C.: Effects of temperature and soil moisture on methyl
947 halide and chloroform fluxes from drained peatland pasture soils, J Environ Monitor, 14, 241-
948 249, 10.1039/c1em10639b, 2012.
949 Kis-Papo, T., Grishkan, I., Oren, A., Wasser, S. P., and Nevo, E.: Spatiotemporal diversity of filamentous
950 fungi in the hypersaline Dead Sea, Mycol Res, 105, 749-756, Doi
951 10.1017/S0953756201004129, 2001.
952 Kotte, K., Low, F., Huber, S. G., Krause, T., Mulder, I., and Scholer, H. F.: Organohalogen emissions from
953 saline environments - spatial extrapolation using remote sensing as most promising tool,
954 Biogeosciences, 9, 1225-1235, 10.5194/bg-9-1225-2012, 2012.
955 Kuyper, B., Palmer, C. J., Labuschagne, C., and Reason, C. J. C.: Atmospheric bromoform at Cape Point,
956 South Africa: an initial fixed-point data set on the African continent, Atmos Chem Phys, 18,
957 5785-5797, 10.5194/acp-18-5785-2018, 2018.
958 Lee-Taylor, J. M., and Holland, E. A.: Litter decomposition as a potential natural source of methyl
959 bromide, J Geophys Res-Atmos, 105, 8857-8864, Doi 10.1029/1999jd901112, 2000.
960 Lenschow, D. H.: Micrometeorological techniques for measuring biosphere-atmosphere trace gas
961 exchange. Biogenic Trace Gases: Measuring Emissions from Soil and Water, P.A. Matson and
962 R.C. Hariss, Eds., Methods in Ecology, Blackwell Science, Oxford, 126-163., 1995.
963 Liu, Y. N., Yvon-Lewis, S. A., Hu, L., Salisbury, J. E., and O'Hern, J. E.: CHBr3, CH2Br2, and CHClBr2 in
964 U.S. coastal waters during the Gulf of Mexico and East Coast Carbon cruise, J Geophys Res-
965 Oceans, 116, Artn C1000410.1029/2010jc006729, 2011.
966 Maier, M., and Schack-Kirchner, H.: Using the gradient method to determine soil gas flux: A review,
967 Agricultural and Forest Meteorology, 192, 78-95, 10.1016/j.agrformet.2014.03.006, 2014.
968 Manley, S. L., and Dastoor, M. N.: Methyl-Iodide (Ch3i) Production by Kelp and Associated Microbes,
969 Marine Biology, 98, 477-482, Doi 10.1007/Bf00391538, 1988.

970 Manley, S. L., Wang, N. Y., Walser, M. L., and Cicerone, R. J.: Coastal salt marshes as global methyl
971 halide sources from determinations of intrinsic production by marsh plants, Global
972 Biogeochem Cy, 20, Artn Gb301510.1029/2005gb002578, 2006.
973 Matveev, V., Peleg, M., Rosen, D., Tov-Alper, D. S., Hebestreit, K., Stutz, J., Platt, U., Blake, D., and
974 Luria, M.: Bromine oxide - ozone interaction over the Dead Sea, J Geophys Res-Atmos, 106,
975 10375-10387, Doi 10.1029/2000jd900611, 2001.
976 Meredith, L. K., Commane, R., Munger, J. W., Dunn, A., Tang, J., Wofsy, S. C., and Prinn, R. G.:
977 Ecosystem fluxes of hydrogen: a comparison of flux-gradient methods, Atmospheric
978 Measurement Techniques, 7, 2787-2805, 10.5194/amt-7-2787-2014, 2014.
979 Moore, R. M., Gut, A., and Andreae, M. O.: A pilot study of methyl chloride emissions from tropical
980 woodrot fungi, Chemosphere, 58, 221-225, 10.1016/j.chemosphere.2004.03.011, 2005.
981 Moore, R. M.: Methyl halide production and loss rates in sea water from field incubation experiments,
982 Mar Chem, 101, 213-219, 10.1016/j.marchem.2006.03.003, 2006.
983 Nadzir, M. S. M., Phang, S. M., Abas, M. R., Rahman, N. A., Abu Samah, A., Sturges, W. T., Oram, D. E.,
984 Mills, G. P., Leedham, E. C., Pyle, J. A., Harris, N. R. P., Robinson, A. D., Ashfold, M. J., Mead, M.
985 I., Latif, M. T., Khan, M. F., Amiruddin, A. M., Banan, N., and Hanafiah, M. M.: Bromocarbons in
986 the tropical coastal and open ocean atmosphere during the 2009 Prime Expedition Scientific
987 Cruise (PESC-09), Atmos Chem Phys, 14, 8137-8148, 10.5194/acp-14-8137-2014, 2014.
988 Niemi, T. M., Ben-Avrahem, Z., and Gat, J.R., : The Dead Sea: The Lake and Its Setting,O xfordM
989 onogr.G eol. Geophys.v, ol. 36, Oxford Univ. Press, New York., 1997.
990 O'Brien, L. M., Harris, N. R. P., Robinson, A. D., Gostlow, B., Warwick, N., Yang, X., and Pyle, J. A.:
991 Bromocarbons in the tropical marine boundary layer at the Cape Verde Observatory -
992 measurements and modelling, Atmos Chem Phys, 9, 9083-9099, 10.5194/acp-9-9083-2009,
993 2009.
994 O'Dowd, C. D., Jimenez, J. L., Bahreini, R., Flagan, R. C., Seinfeld, J. H., Hameri, K., Pirjola, L., Kulmala,
995 M., Jennings, S. G., and Hoffmann, T.: Marine aerosol formation from biogenic iodine
996 emissions, Nature, 417, 632-636, DOI 10.1038/nature00775, 2002.
997 Obrist, D., Tas, E., Peleg, M., Matveev, V., Fain, X., Asaf, D., and Luria, M.: Bromine-induced oxidation
998 of mercury in the mid-latitude atmosphere, Nature Geoscience, 4, 22-26, 10.1038/Ngeo1018,
999 2011.
1000 Oren, A., and Shilo, M.: Factors Determining the Development of Algal and Bacterial Blooms in the
1001 Dead-Sea - a Study of Simulation Experiments in Outdoor Ponds, Fems Microbiol Ecol, 31, 229-
1002 237, 1985.
1003 Oren, A., Ionescu, D., Hindiyeh, M., and Malkawi, H.: Microalgae and cyanobacteria of the Dead Sea
1004 and its surrounding springs, Isr J Plant Sci, 56, 1-13, Doi 10.1560/Ijps.56.1-2.1, 2008.
1005 Osman, K. T.: Forest soils: properties and management. In 'Physical properties of forest soils', 19–28,
1006 2013.
1007 Pasquill, F., and Smith, F. B.: The physical and meteorological basis for the estimation of the dispersion
1008 of windborn material, in (H. M. Englund and W. T. Beery, Eds.), Proceedings of the Second
1009 International Clean Air Congress, Washington, DC, 1970, pp. 1067-1072, Academic Press, New
1010 York, , 1971.
1011 Pedersen, M., Collen, J., Abrahamsson, K., and Ekdahl, A.: Production of halocarbons from seaweeds:
1012 An oxidative stress reaction?, Scientia Marina, 60, 257-263, 1996.
1013 Pen-Mouratov, S., Myblat, T., Shamir, I., Barness, G., and Steinberger, Y.: Soil Biota in the Arava Valley
1014 of Negev Desert, Israel, Pedosphere, 20, 273-284, Doi 10.1016/S1002-0160(10)60015-X, 2010.
1015 Pyle, J. A., Ashfold, M. J., Harris, N. R. P., Robinson, A. D., Warwick, N. J., Carver, G. D., Gostlow, B.,
1016 O'Brien, L. M., Manning, A. J., Phang, S. M., Yong, S. E., Leong, K. P., Ung, E. H., and Ong, S.:
1017 Bromoform in the tropical boundary layer of the Maritime Continent during OP3, Atmos Chem
1018 Phys, 11, 529-542, 10.5194/acp-11-529-2011, 2011.
1019 Quack, B., and Wallace, D. W. R.: Air-sea flux of bromoform: Controls, rates, and implications (vol 17,
1020 art no 1023, 2003), Global Biogeochem Cy, 18, Artn Gb100410.1029/2003gb002187, 2004.
1021 Rhew, R. C., Miller, B. R., and Weiss, R. F.: Natural methyl bromide and methyl chloride emissions from
1022 coastal salt marshes, Nature, 403, 292-295, Doi 10.1038/35002043, 2000.

Rhew, R. C., Miller, B. R., Vollmer, M. K., and Weiss, R. F.: Shrubland fluxes of methyl bromide and methyl chloride, J Geophys Res-Atmos, 106, 20875-20882, Doi 10.1029/2001jd000413, 2001.

Rhew, R. C., Miller, B. R., Bill, M., Goldstein, A. H., and Weiss, R. F.: Environmental and biological controls on methyl halide emissions from southern California coastal salt marshes, Biogeochemistry, 60, 141-161, Doi 10.1023/A:1019812006560, 2002.

Rhew, R. C., Aydin, M., and Saltzman, E. S.: Measuring terrestrial fluxes of methyl chloride and methyl bromide using a stable isotope tracer technique, Geophys Res Lett, 30, Artn 2103 10.1029/2003gl018160, 2003.

Rhew, R. C., Teh, Y. A., Abel, T., Atwood, A., and Mazeas, O.: Chloroform emissions from the Alaskan Arctic tundra, Geophys Res Lett, 35, Artn L2181110.1029/2008gl035762, 2008.

Rhew, R. C., Whelan, M. E., and Min, D. H.: Large methyl halide emissions from south Texas salt marshes, Biogeosciences, 11, 6427-6434, 10.5194/bg-11-6427-2014, 2014.

Rousseaux, M. C., Ballare, C. L., Giordano, C. V., Scopel, A. L., Zima, A. M., Szwarcberg-Bracchitta, M., Searles, P. S., Caldwell, M. M., and Diaz, S. B.: Ozone depletion and UVB radiation: Impact on plant DNA damage in southern South America, Proceedings of the National Academy of Sciences of the United States of America, 96, 15310-15315, DOI 10.1073/pnas.96.26.15310, 1999.

Ruecker, A., Weigold, P., Behrens, S., Jochmann, M., Laaks, J., and Kappler, A.: Predominance of Biotic over Abiotic Formation of Halogenated Hydrocarbons in Hypersaline Sediments in Western Australia, Environ Sci Technol, 48, 9170-9178, 10.1021/es501810g, 2014.

Schmugge, T. j., and André, J.-C.: Land surface evaporation: measurement and parameterization: Springer Science & Business Media, 1991.

Simmonds, P. G., Derwent, R. G., Manning, A. J., O'Doherty, S., and Spain, G.: Natural chloroform emissions from the blanket peat bogs in the vicinity of Mace Head, Ireland over a 14-year period, Atmos Environ, 44, 1284-1291, 10.1016/j.atmosenv.2009.12.027, 2010.

Simpson, W. R., Brown, S. S., Saiz-Lopez, A., Thornton, J. A., and von Glasow, R.: Tropospheric Halogen Chemistry: Sources, Cycling, and Impacts, Chemical Reviews, 115, 4035-4062, 10.1021/cr5006638, 2015.

Sive, B. C., Varner, R. K., Mao, H., Blake, D. R., Wingenter, O. W., and Talbot, R.: A large terrestrial source of methyl iodide, Geophys Res Lett, 34, Artn L1780810.1029/2007gl030528, 2007.

Stull , R. B.: An introduction to boundary layer meteorology. Kluwer, Dordrecht 1988.

Sverdrup, H. U., Johnson, M.W., and Fleming, R.H.,: The Oceans, Their Physics, Chemistry and General Biology, Prentice-Hall, Englewood Cliffs, N.J., 1942.

Tas, E., Matveev, V., Zingler, J., Luria, M., and Peleg, M.: Frequency and extent of ozone destruction episodes over the Dead Sea, Israel, Atmos Environ, 37, 4769-4780, 10.1016/j.atmosenv.2003.08.015, 2003.

Tas, E., Peleg, M., Matveev, V., Zingler, J., and Luria, M.: Frequency and extent of bromine oxide formation over the Dead Sea, J Geophys Res-Atmos, 110, Artn D1130410.1029/2004jd005665, 2005.

Tas, E., Peleg, M., Pedersen, D. U., Matveev, V., Biazar, A. P., and Luria, M.: Measurement-based modeling of bromine chemistry in the boundary layer: 1. Bromine chemistry at the Dead Sea, Atmos Chem Phys, 6, 5589-5604, 2006.

Tas, E., Obrist, D., Peleg, M., Matveev, V., Fain, X., Asaf, D., and Luria, M.: Measurement-based modelling of bromine-induced oxidation of mercury above the Dead Sea, Atmos Chem Phys, 12, 2429-2440, 10.5194/acp-12-2429-2012, 2012.

Varner, R. K., Crill, P. M., and Talbot, R. W.: Wetlands: a potentially significant source of atmospheric methyl bromide and methyl chloride, Geophys Res Lett, 26, 2433-2435, Doi 10.1029/1999gl900587, 1999.

Warwick, N. J., Pyle, J. A., and Shallcross, D. E.: Global modelling of the atmospheric methyl bromide budget, J Atmos Chem, 54, 133-159, 10.1007/s10874-006-9020-3, 2006.

Watling, R., and Harper, D. B.: Chloromethane production by wood-rotting fungi and an estimate of the global flux to the atmosphere, Mycol Res, 102, 769-787, Doi 10.1017/S0953756298006157, 1998.

1076 Weissflog, L., Lange, C. A., Pfennigsdorff, A., Kotte, K., Elansky, N., Lisitzyna, L., Putz, E., and Krueger,
1077 G.: Sediments of salt lakes as a new source of volatile highly chlorinated C1/C2 hydrocarbons,
1078 Geophys Res Lett, 32, Artn L0140110.1029/2004gl020807, 2005.
1079 Wishkerman, A., Gebhardt, S., McRoberts, C. W., Hamilton, J. T. G., Williams, J., and Keppler, F.:
1080 Abiotic methyl bromide formation from vegetation, and its strong dependence on
1081 temperature, Environ Sci Technol, 42, 6837-6842, 10.1021/es800411j, 2008.
1082 WMO, W. M. O.: Guide to Meteorological Instruments and Methods of Observation, 2008.
1083 Xiao, X., Prinn, R. G., Fraser, P. J., Simmonds, P. G., Weiss, R. F., O'Doherty, S., Miller, B. R., Salameh, P.
1084 K., Harth, C. M., Krummel, P. B., Porter, L. W., Muhle, J., Greally, B. R., Cunnold, D., Wang, R.,
1085 Montzka, S. A., Elkins, J. W., Dutton, G. S., Thompson, T. M., Butler, J. H., Hall, B. D., Reimann,
1086 S., Vollmer, M. K., Stordal, F., Lunder, C., Maione, M., Arduini, J., and Yokouchi, Y.: Optimal
1087 estimation of the surface fluxes of methyl chloride using a 3-D global chemical transport
1088 model, Atmos Chem Phys, 10, 5515-5533, 10.5194/acp-10-5515-2010, 2010.
1089 Yang, K., Tamai, N., and Koike, T.: Analytical solution of surface layer similarity equations, J Appl
1090 Meteorol, 40, 1647-1653, Doi 10.1175/1520-0450(2001)040<1647:Asosls>2.0.Co;2, 2001.
1091 Yassaa, N., Wishkerman, A., Keppler, F., and Williams, J.: Fast determination of methyl chloride and
1092 methyl bromide emissions from dried plant matter and soil samples using HS-SPME and GC-
1093 MS: method and first results, Environmental Chemistry, 6, 311-318, 10.1071/En09034, 2009.
1094 Yokouchi, Y., Ikeda, M., Inuzuka, Y., and Yukawa, T.: Strong emission of methyl chloride from tropical
1095 plants, Nature, 416, 163-165, DOI 10.1038/416163a, 2002.
1096 Yokouchi, Y., Inagaki, T., Yazawa, K., Tamaru, T., Enomoto, T., and Izumi, K.: Estimates of ratios of
1097 anthropogenic halocarbon emissions from Japan based on aircraft monitoring over Sagami
1098 Bay, Japan, J Geophys Res-Atmos, 110, Artn D06301
1099 10.1029/2004jd005320, 2005.
1100 Yokouchi, Y., Saito, T., Ishigaki, C., and Aramoto, M.: Identification of methyl chloride-emitting plants
1101 and atmospheric measurements on a subtropical island, Chemosphere, 69, 549-553,
1102 10.1016/j.chemosphere.2007.03.028, 2007.
1103 Zhou, Y., Mao, H. T., Russo, R. S., Blake, D. R., Wingenter, O. W., Haase, K. B., Ambrose, J., Varner, R.
1104 K., Talbot, R., and Sive, B. C.: Bromoform and dibromomethane measurements in the seacoast
1105 region of New Hampshire, 2002-2004, J Geophys Res-Atmos, 113, Artn D08305
1106 10.1029/2007jd009103, 2008.
1107 Zingler, J., and Platt, U.: Iodine oxide in the Dead Sea Valley: Evidence for inorganic sources of
1108 boundary layer IO, J Geophys Res-Atmos, 110, Artn D0730710.1029/2004jd004993, 2005.
1109 Ziska, F., Quack, B., Abrahamsson, K., Archer, S. D., Atlas, E., Bell, T., Butler, J. H., Carpenter, L. J.,
1110 Jones, C. E., Harris, N. R. P., Hepach, H., Heumann, K. G., Hughes, C., Kuss, J., Kruger, K., Liss, P.,
1111 Moore, R. M., Orlikowska, A., Raimund, S., Reeves, C. E., Reifenhauser, W., Robinson, A. D.,
1112 Schall, C., Tanhua, T., Tegtmeier, S., Turner, S., Wang, L., Wallace, D., Williams, J., Yamamoto,
1113 H., Yvon-Lewis, S., and Yokouchi, Y.: Global sea-to-air flux climatology for bromoform,
1114 dibromomethane and methyl iodide, Atmos Chem Phys, 13, 8915-8934, 10.5194/acp-13-8915-
1115 2013, 2013.
1116